Dynamics of the Heisenberg Ferromagnet at Low Temperatures*

RICHARD SILBERGLITT† AND A. BROOKS HARRIS‡
Department of Physics, University of Pennsylvania, Philadelphia, Pennsylvania 19104
(Received 19 April 1968)

Dyson calculated the effect of spin-wave interactions on the static (thermodynamic) properties of the Heisenberg ferromagnet. Within the same approximation, that of including only the contributions of lowest-order (two-magnon) scattering processes and neglecting the kinematic interaction, we have calculated the dynamic properties of this system and find results consistent with Dyson's in the zero-wave-vector limit. In the short-wavelength limit where perturbation theory diverges, we discuss nonperturbatively via the t matrix the influence of the two-spin-wave bound states and the two-spin-wave resonant scattering states on the single-particle spectrum as characterized by the transverse spectral weight function $A_k(\omega)$. We find that although the total cross section of the bound states is too small for them to be observed directly, the anomalous effect of the bound states and resonant scattering states on the renormalization of the spin-wave energy is observable under favorable conditions. In general, we find the quasiparticle picture to be valid; however, at the highest temperature considered the resonant scattering states cause an extra resonance in the susceptibility. Most of the results for $A_k(\omega)$ are given numerically and have been checked against the sum rules, although the energy shift and energy width as deduced from $\Sigma_k(\epsilon_k)$ are given analytically by rather simple expressions. We have obtained for the first time a Green's function that is capable of yielding correctly at low temperatures both the static and dynamic properties for arbitrary spin.

I. INTRODUCTION

THE Heisenberg model of ferromagnetism has been extensively studied since its proposal in 1926.[1] Bloch was the first to point out that the elementary excitations from the fully aligned ground state are the coherent reversals of magnetic moments smeared out over the crystal in a wavelike manner.[2] He also calculated the effect of these spin-wave excitations, or magnons, on the thermodynamic properties within the approximation that the excitations do not interact with one another. This type of calculation was extended and systematized by Holstein and Primakoff[3] via the introduction of a transformation from spin operators to boson operators. They were thus able to write down the terms in the equivalent boson Hamiltonian responsible for the interaction between magnons. From their arguments it is clear that the simple Bloch theory becomes exact either at low temperatures as the thermal average number of magnons goes to zero, or for infinite spin where the interactions vanish.

Several authors subsequently attempted to improve on the Holstein-Primakoff treatment by expanding the square roots introduced by the transformation from spin to boson operators and treating the nonquadratic parts perturbatively.[4,5] Because the interaction between the Holstein-Primakoff spin-waves is large even for long wavelength, one must group the terms together properly,[6] as for instance, according to powers of $1/S$ and $\langle n\rangle$, where S is the spin and $\langle n\rangle$ the density of magnons. This problem was overcome by Dyson,[7] who introduced a simple equivalent boson Hamiltonian that consisted of terms quadratic and quartic in the boson operators. He was then able to sum explicitly the perturbation series for the free energy, including terms of all orders in $1/S$ that are of leading nontrivial order in $\langle n\rangle$. Furthermore, he was able to conclude that perturbative calculations for static thermodynamic quantities were qualitatively correct over a wide temperature interval, say, $T/T_c<\frac{1}{2}$. Actually because of the weakness of the long-wavelength interactions the expansion parameter turns out to be $\langle n\rangle(k_BT/4JS)$ rather than $\langle n\rangle$.

Dyson also pointed out that calculation of the properties of a low-density gas of magnons is formally identical to that for any low-density system of weakly interacting particles. By weakly interacting, one means that there are no low-energy two-particle bound states. In other words, the thermodynamically important two-particle, i.e., two-spin-deviation, states are those that do not differ qualitatively from the states of two noninteracting particles. Although Dyson did not investigate the possible occurrence of bound states in full detail, he showed that even if they did exist, they would not affect the low-temperature thermodynamics. A more complete analysis of the two-spin-wave states has since been carried out by Wortis.[8] He found that bound states of two spin-waves do indeed exist for the c.m. momentum $\mathbf{k}$ greater than a critical value k_c, the exact value depending on the direction of $\mathbf{k}$ in reciprocal space.

The problem of the interactions of two spin-waves is quite similar to the usual two-body problem,[9] except that in the c.m. system the resulting potential depends on the c.m. momentum. The analogous situation in

* Supported in part by the Advanced Research Projects Agency and the National Science Foundation under Grant No. GP-6771.
† National Aeronautics and Space Administration Predoctoral Fellow. Present address: Department of Physics, University of California, Santa Barbara, Calif.
‡ Alfred P. Sloan Postdoctoral Fellow.
[1] W. Heisenberg, Z. Physik **38**, 411 (1926).
[2] F. Bloch, Z. Physik **61**, 206 (1930).
[3] T. Holstein and H. Primakoff, Phys. Rev. **58**, 1098 (1940).
[4] M. R. Schafroth, Proc. Phys. Soc. (London) **A67**, 33 (1954).
[5] J. Van Kranendonk, Physica **21**, 91 (1955).
[6] T. Oguchi, Phys. Rev. **117**, 117 (1960).
[7] F. J. Dyson, Phys. Rev. **102**, 1217, 1230 (1956).
[8] M. Wortis, Phys. Rev. **132**, 85 (1963).
[9] P. Roman, *Advanced Quantum Theory* (Addison-Wesley Publishing Company, Inc., Reading, Mass., 1965).

potential scattering is the scattering of a particle from a spherical potential well whose depth, for the purposes of the analogy, is dependent on the total momentum of the two spin-waves. For very shallow wells, only a continuum of scattering states exist. As the well becomes deeper one finds the emergence of a bound state. Continuing the process, one finds successively more bound states as the depth of the well is increased. For small c.m. momentum, one is in the regime where only scattering states exist. Towards the edge of the Brillouin zone, the momentum-dependent attractive potential is strong enough to support one, two, and finally three bound states of two spin-waves.

An interesting aspect of the two-spin-wave problem has been discussed by Boyd and Callaway.[10] They resolve the scattering cross section into its partial-wave components and show that there are both s-wave and d-wave bound states. In addition, they point out that for k of the order of, but less than, k_c, that is, when the potential is not quite strong enough to support a bound state, the d-wave (but not the s-wave) states connect to a set of resonant scattering states. In these states, the two spin-waves may be thought of as interacting so strongly that they undergo several successive collisions before separating. The resonant states are analogous to those found in the scattering of a particle from a spherical potential well that posesses a barrier, such as the angular momentum barrier $l(l+1)/r^2$. In this case, the wave function is peaked inside the well, decays exponentially within the barrier, and then takes on free-particle character outside. In the two-spin-wave problem the barrier arises in the following manner. Consider the phase relation between spins on a large sphere about the scattering site. Since an s-wave bound state must be spherically symmetric, all these spins are in phase and there is no exchange energy associated with such a configuration. However, for a d-wave state there must be two nodes in the phase wave function and thus neighboring spins will be out of phase. Therefore the d configuration has exchange energy associated with it. Moreover, as one decreases the radius of the sphere, the phase variation becomes more rapid and the associated exchange energy increases. This increase in the energy of the d configuration with decreasing radius from the scattering site is equivalent to a potential barrier, and explains why there are resonant d states but no resonant s states.

One expects that rather dramatic effects on the single-particle states are possible, when the energy of a resonant state or "quasi-bound state" is equal to that of the single-particle excitation of the same momentum. Under this condition one expects that the single-particle excitation, or magnon, may combine with a long-wavelength thermal magnon and be in resonance with the quasi-bound state. This phenomenon is the perfectly general and familiar one of level crossing in quantum mechanics. A typical example of this in magnetism is the effect of magnon-phonon interaction on the crossover of the magnon and phonon dispersion curves.[11] In the present case, the resonance is not between two different single-particle excitations (magnons and phonons) but rather between a single-particle excitation, magnon, and a two-particle excitation, the quasi-bound state. Accordingly, a better analogy is to be made with the Berk-Schrieffer theory of spin fluctuations in nearly ferromagnetic metals.[12] In that case, although one does not have two-particle bound states (of electron-hole pairs), the large susceptibility is indicative of paramagnons, which are just quasi-bound states of electrons and holes of opposite spin in exactly the sense we have discussed for the spin-wave bound states. As Berk and Schrieffer show, the severe interaction with the paramagnons causes the single-particle excitations to be strongly modified. Thus they explain the large electron effective-mass enhancement in nearly ferromagnetic metals. Our results are quite similar to theirs in that we find an anomaly in the magnon renormalization when the magnon energy approaches the energy of the quasi-bound states. An important difference between the two physical situations is that, whereas in the case of nearly ferromagnetic metals one can observe the quasi-bound states directly through the large paramagnetic susceptibility, in the case of two-spin-wave bound states it is difficult to couple directly to them via an external field, thus making their direct observation difficult (although it may be possible, as we point out in Sec. IV). However, their indirect observation via their effect on the magnon spectrum should be more feasible through inelastic neutron-scattering experiments.

It is clear that in order to study such effects perturbation theory is hopelessly inadequate. What one must do is to construct the analog of Dyson's theory as applied to the calculation of the dynamical properties. Previous authors have obtained formal expressions which would describe this effect, and have evaluated the magnon renormalization for small wave vectors.[13–15]

[10] R. G. Boyd and J. Callaway, Phys. Rev. **138**, A1621 (1965).

[11] P. Erdös, Phys. Rev. **139**, A1249 (1965).

[12] N. F. Berk and J. R. Schrieffer, Phys. Rev. Letters **17**, 433 (1966).

[13] For $ak \ll 1$ but $\epsilon_k \gg k_BT$, expressions for the energy renormalization, including damping, may be deduced from Dyson's results (Ref. 7) for the thermodynamics and cross section. These results have been rederived within a Green's-function formalism by V. N. Kashcheev and M. A. Krivoglaz, Fiz. Tverd. Tela **3**, 1541 (1961) [English transl.: Soviet Phys.—Solid State **3**, 1117 (1961)]; R. A. Tahir-Kheli and D. ter Haar, Phys. Rev. **127**, 95 (1962); J. F. Cooke and H. A. Gersch, *ibid.* **153**, 641 (1967); W. Marshall and G. Murray, J. Appl. Phys. **39**, 380 (1968).

[14] For $ak \ll 1$ and $\epsilon_k \ll k_BT$, the damping has been evaluated by Kashcheev and Krivoglaz, and a valid expression was also given by Tahir-Kheli and ter Haar. The contradictory results given by Cooke and Gersch and by Marshall and Murray are believed to be in error, and this will be discussed more fully in a subsequent paper.

[15] For $ak \ll 1$ anisotropy also contributes to the damping. This case is discussed by S. V. Peletminskii and V. G. Bar'yakhtar, Fiz. Tverd. Tela **6**, 219 (1964) [English transl.: Soviet Phys.—Solid State **6**, 174 (1964)].

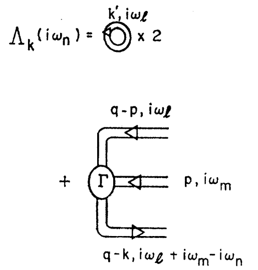

FIG. 1. The diagrammatic expansion for $\Lambda_k(i\omega_n)$, the function which determines the difference between the spin and boson Green's functions through Eq. (14).

For large wave vectors these complicated expressions are rather unenlightening, and to our knowledge no one has previously pointed out the possible effects of the quasi-bound states on the single-particle spectrum. By confining our attention to the [111] direction in reciprocal space we were able to obtain simplified expressions whose evaluation was reported previously.[16] The purpose of this paper is to give a more complete description of the physics and mathematics of the theory.

Briefly, this paper is organized as follows: In Sec. II we formulate the problem; in Sec. III we outline the low-density expansion to be used; in Sec. IV we describe and interpret our results. Finally, in Sec. V we draw some conclusions from our calculations.

II. PROBLEM FORMULATION

The Hamiltonian of an ideal isotropic Heisenberg ferromagnet with nearest-neighbor interactions is

$$\mathcal{H}_{\rm Heis}=-J\sum_{\langle i,j\rangle}\mathbf{S}_i\cdot\mathbf{S}_j, \tag{1}$$

where J is a positive constant and the sum extends over all nearest-neighbor pairs in a simple cubic lattice. We shall employ the Dyson-Maléev (DM) representation[7,17] for the spin operators, given by

$$S_i^+=(2S)^{1/2}a_i^\dagger(1-a_i^\dagger a_i/2S), \tag{2a}$$

$$S_i^-=(2S)^{1/2}a_i, \tag{2b}$$

$$S_i^z=a_i^\dagger a_i-S, \tag{2c}$$

where a_i and $a_i^\dagger$ destroy and create, respectively, bosons at the site i. In terms of this representation, the Hamiltonian (1) becomes[18]

$$\mathcal{H}_{\rm DM}=E_0+\sum_k\epsilon_k a_k^\dagger a_k-\frac{Jz}{2N}\sum_{pkq}\Gamma_{pkq}a_{k+q}^\dagger a_{p-q}^\dagger a_p a_k, \tag{3a}$$

$$\Gamma_{pkq}=\tfrac{1}{2}(\gamma_q+\gamma_{k+q-p}-\gamma_p-\gamma_k), \tag{3b}$$

$$\gamma_k=z^{-1}\sum_\delta \exp(i\mathbf{k}\cdot\boldsymbol{\delta}), \tag{3c}$$

where

$$E_0=-\tfrac{1}{2}JNzS^2, \tag{4a}$$

$$\epsilon_k=JzS(1-\gamma_k). \tag{4b}$$

Here N is the number of lattice sites, E_0 is the ground-state energy of the system, and ϵ_k is the energy of a single spin wave in the free-particle approximation. In Eq. (3a), $\boldsymbol{\delta}$ is a vector from a lattice site to one of its z nearest neighbors ($z=6$ for the simple cubic case we treat), and

$$a_k=N^{-1/2}\sum_{\mathbf{x}_i}\exp(i\mathbf{k}\cdot\mathbf{x}_i)a_i. \tag{5}$$

The boson Hamiltonian (3a) consists of a kinetic-energy term (corresponding to a gas of simple spin waves) and a two-body momentum-conserving potential, which represents the interactions between spin waves. The potential is of the standard form, with two exceptions. First, it is nonlocal, so that Γ_{pkq} depends not only on the momentum transfer $\mathbf{q}$ but also on the incoming momenta $\mathbf{p}$ and $\mathbf{k}$. Second, $\mathcal{H}_{\rm DM}$ is non-Hermitian. Neither of these facts causes any calculational problem, since one may still use all of the formulas of Feynman diagrammatic perturbation theory, being careful nowhere to assume $V=V^\dagger$ and remembering that Γ_{pkq} is not just $\Gamma(q)$ as one usually finds. Finally, we note that the local part of the effective interaction between spin waves, i.e., that from terms involving S_z operators, is attractive.

We wish to calculate the transverse component of the dynamical susceptibility, which is the linear response function of the system. The transverse susceptibility is the spin Green's function

$$\chi(\mathbf{k},\omega)=-i(g\mu_B)^2\int_{-\infty}^{\infty}dt\, e^{i\omega t}\Theta(t)\langle[S_k^-(t),S_k^+(0)]\rangle, \tag{6}$$

in the usual notation and possesses the spectral representation[19]

$$\chi(\mathbf{k},\omega)=-(g\mu_B)^2\int_{-\infty}^{\infty}d\omega'\frac{A_k(\omega')}{\omega'-\omega-i\delta}\qquad(\delta\to0^+), \tag{7}$$

[16] R. Silberglitt and A. B. Harris, Phys. Rev. Letters **19**, 30 (1967).
[17] S. V. Maléev, Zh. Eksperim. i Teor. Fiz. **33**, 1010 (1957) [English transl.: Soviet Phys.—JETP **6**, 776 (1956)].
[18] In this equation all wave vectors are restricted to the first Brillouin zone of the reciprocal lattice. Actually the potential should contain a Kronecker δ conserving momentum only up to a reciprocal lattice vector, but due to the periodicity of all functions we deal with (including the t matrix), use of (3a) properly describes the system, including the contribution of all umklapp processes by bringing all vectors back to the first zone. One cannot make such an argument for a many-sublattice system.
[19] D. N. Zubarev, Usp. Fiz. Nauk **71**, 71 (1960) [English transl.: Soviet Phys.—Usp. **3**, 320 (1960)].

where the spectral weight function $A_k(\omega)$ is given by

$$A_k(\omega)=Z^{-1}\sum_{m,n}[\exp(-\beta E_m)-\exp(-\beta E_n)]\,|\langle n\mid S_k^+\mid m\rangle|^2\delta(\omega-E_n+E_m). \tag{8}$$

Here Z is the partition function and $|m\rangle$ and $|n\rangle$ are exact eigenstates of $\mathcal{H}_{\mathrm{Heis}}$. This function contains all important physical information about the spin-wave excitation spectrum of the system at finite temperature, since $A_k(\omega)/(1-e^{-\beta\omega})$ for positive ω is the probability of exciting a transverse excitation of momentum $\mathbf{k}$ and energy ω in the system. In fact, the inelastic neutron-scattering cross section is given directly in terms of $A_k(\omega)$.[20] It is also true that from the spectral weight function one may determine both the real and imaginary parts of the susceptibility, through the relations

$$-\pi(g\mu_B)^2A_k(\omega)=\operatorname{Im}\chi(\mathbf{k},\omega), \tag{9a}$$

$$\operatorname{Re}\chi(\mathbf{k},\omega)=\pi^{-1}P\int_{-\infty}^{\infty}d\omega'\,\frac{\operatorname{Im}\chi(\mathbf{k},\omega')}{\omega'-\omega}. \tag{9b}$$

Thus $A_k(\omega)$ gives a rather complete description of the dynamics of the system. In Sec. III we will show how to calculate it for all $\mathbf{k}$ and ω at low temperatures. Numerical results of the calculations will then be displayed and interpreted in Sec. IV.

In our calculations we will utilize the Green's function

$$\mathcal{G}_k^S(\tau)=-\langle T_\tau S_k^-(\tau)S_k^+(0)\rangle, \tag{10a}$$

$$S_k^-(\tau)=\exp(\mathcal{H}_{\mathrm{DM}}\tau)S_k^-\exp(-\mathcal{H}_{\mathrm{DM}}\tau), \tag{10b}$$

and its Fourier transform

$$\mathcal{G}_k^S(i\omega_n)=\int_0^\beta d\tau\,\exp(i\omega_n\tau)\mathcal{G}_k^S(\tau), \tag{11}$$

where

$$\omega_n=2\pi n/\beta \qquad (n\text{ an integer}). \tag{12}$$

These Green's functions have been very well studied and their properties have been discussed extensively in the literature.[19,21,22] It is well known that $\mathcal{G}_k^S(i\omega_n)$ possesses the spectral representation

$$\mathcal{G}_k^S(i\omega_n)=-\int_{-\infty}^{\infty}d\omega'\,\frac{A_k(\omega')}{\omega'-i\omega_n}, \tag{13a}$$

$$A_k(\omega)=-\pi^{-1}\operatorname{Im}\mathcal{G}_k^S(\omega+i\delta) \qquad (\delta\to0^+), \tag{13b}$$

where $A_k(\omega)$ is given by Eq. (8), so that the imaginary part of this Green's function gives the spectral weight function of the finite-temperature susceptibility. Writing the spin operators in Eq. (10) in terms of bosons through the use of Eq. (2), and neglecting kinematic effects (see Appendix A), we find that the spin Green's function involves both the one- and the two-particle boson Green's functions. It has been shown,[15] however, that for this system the two-particle boson Green's function equals a function of momentum and frequency times the single-particle boson function. Thus we obtain from Eqs. (2), (10), and (11)

$$\mathcal{G}_k^S(i\omega_n)=2S\mathcal{G}_k(i\omega_n)\{1+[\Lambda_k(i\omega_n)/2S]\}, \tag{14}$$

where

$$\mathcal{G}_k(i\omega_n)=[i\omega_n-\epsilon_k-\Sigma_k(i\omega_n)]^{-1} \tag{15}$$

is the boson Green's function, $\Sigma_k(i\omega_n)$ is the usual irreducible boson self-energy, and $\Lambda_k(i\omega_n)$ is given diagrammatically in Fig. 1. In Fig. 1, the double lines represent $\mathcal{G}_k(i\omega_n)$ and Γ is a vertex function, the sum of the internal parts of all diagrams with two solid lines both coming in and going out. Note that in lowest order lambda is just $\Lambda^{(1)}=-2\langle n\rangle$, so that the boson and spin Green's functions differ by a factor of

$$1-\langle n\rangle/S\approx-\langle S^z\rangle/S.$$

In terms of $\Sigma_k(\omega)$ and $\Lambda_k(\omega)$ the spectral weight function is given by

$$A_k(\omega)=-(2S/\pi)\lim_{\delta\to0^+}|\omega-\epsilon_k-\Sigma_k(\omega)+i\delta|^{-2}\times\{(\Sigma_k''(\omega)+[(\omega-\epsilon_k+i\delta)/2S]\Lambda_k''(\omega))$$
$$-\operatorname{Im}[(2S)^{-1}\Sigma_k^*(\omega)\Lambda_k(\omega)]-\delta[1+(2S)^{-1}\Lambda_k'(\omega)]\}, \tag{16}$$

where a prime denotes the real part and a double prime denotes the imaginary part; here $\Sigma_k(i\omega_n)$ and $\Lambda_k(i\omega_n)$ are understood to be evaluated for ω just above the real axis. In Sec. III we discuss the low-temperature approximations for $\Sigma_k(\omega)$ and $\Lambda_k(\omega)$ and derive in terms of them a more compact expression for $A_k(\omega)$ from Eq. (16). As is discussed in Appendix D, this expression also gives a spectral weight function from which one can obtain thermodynamic quantities consistent with Dyson's[7] results to all orders in $1/S$.

III. LOW-DENSITY APPROXIMATION

At low temperatures we will employ the diagrammatic density expansions for $\Sigma_k(\omega)$ and $\Lambda_k(\omega)$. The

[20] L. Van Hove, Phys. Rev. **95**, 249 (1954); **95**, 1374 (1954).

[21] T. Matsubara, Progr. Theoret. Phys. (Kyoto) **14**, 351 (1955).

[22] A. A. Abrikosov, L. P. Gorkov, and I. Y. Dzyaloshinskii, *Quantum Field Theoretical Methods in Statistical Physics* (Pergamon Press, Inc., New York, 1965), 2nd ed.

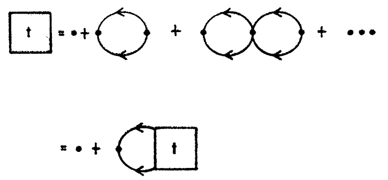

FIG. 2. The t matrix, or sum of ladder diagrams, which appears in the one-backward-line approximations for $\Sigma_k(i\omega_n)$ and $\Lambda_k(i\omega_n)$.

rules for calculating $\Sigma_k(\omega)$ have been given by a number of authors[23–25]; most notable is Ref. 25, where an explicit derivation of the general term is given. The generalization of the rules necessary for a diagrammatic calculation of $\Lambda_k(\omega)$ is straightforward. In the Baym-Sessler formalism the Matsubara sums for a diagram with n vertices are performed by associating with each original diagram the set of $n!$ "time-ordered" diagrams obtained by considering all possible time orderings of the vertices. In this formulation each line of momentum **k** running backward in time is a hole line carrying the factor n_k and each line running forward in time is a particle line carrying a factor $1+n_k$, where $n_k\equiv[\exp(\beta\epsilon_k)-1]^{-1}$. Thus a classification of diagrams according to the number of backward lines leads naturally to an expansion in the density of quasiparticles. Dyson[7] has shown that summing the first two terms in the density expansion yields the magnetization correctly to order T^4. This corresponds to including all two-particle scattering processes or (for dynamical quantities) all one-backward-line diagrams. Consequently, we will sum all contributions to $\Sigma_k(\omega)$ and $\Lambda_k(\omega)$ with at most one backward line and will find that the errors thus incurred are at most of order T^5.

The one-backward-line approximations for $\Sigma_k(\omega)$ and $\Lambda_k(\omega)$ are given in terms of the t matrix, or sum of ladder diagrams, shown in Fig. 2. Diagrammatic expressions for $\Sigma_k(\omega)$ and $\Lambda_k(\omega)$ in terms of t are shown in Fig. 3. Note that the backward line appearing in both expressions is one of the *outgoing* lines of the t matrix. One of the properties of Γ_{pkq} given by Eq. (3b) is that it vanishes if either of the outgoing lines has zero momentum ($\mathbf{p}=\mathbf{q}$ or $\mathbf{k}=-\mathbf{q}$). From Fig. 2, or Eq. (20), it is clear that the t matrix also has this property, since the dot carries a factor $Jz\Gamma_{pkq}$. Thus the t-matrix terms in Fig. 3 both involve integrals over **p** of n_p times t, where **p** is the momentum of one of the outgoing lines of the t matrix. Since $n_p=[\exp(\beta\epsilon_p)-1]^{-1}$, the main contribution to the integral comes from small **p**. Converting to the dimensionless variable $x=(\beta JSp)^{1/2}$, we see that each factor of p_i in the integrand gives a factor of $T^{1/2}$ (hence $\sum_p n_p\approx T^{3/2}$). Due to the vanishing of t for $\mathbf{p}=0$ and the fact that n_p is an even function of **p**, we find that the lowest-order contribution to the integral n_p times t is of order $\sum_p n_p p^2$, or $T^{5/2}$. Making the definition

$$\Lambda^{(1)}=-(2/N)\sum_p n_p=-2n, \tag{17}$$

we observe that both $\Sigma_k(\omega)$ and $\Lambda_k(\omega)-\Lambda^{(1)}$ are in lowest order proportional to $T^{5/2}$. This result for $\Sigma_k(\omega)$ verifies that we will obtain the correct low-temperature renormalization of the spin-wave energies "with the internal energy" rather than "with the magnetization."

We now return to the expression for the spectral weight function in terms of $\Sigma_k(\omega)$ and $\Lambda_k(\omega)$, Eq. (16). Retaining only the leading term in the numerator, which is of order $T^{5/2}$, we obtain

$$A_k(\omega)=-\frac{2S}{\pi}\frac{\mathrm{Im}R_k(\omega)}{|\omega-\epsilon_k-\Sigma_k(\omega)+i\delta|^2}, \tag{18}$$

where

$$R_k(\omega)=\Sigma_k(\omega)+(1/2S)(\omega-\epsilon_k+i\delta)\Lambda_k(\omega). \tag{19}$$

We neglected the second term on the right-hand side of Eq. (16) because it consists of $(2S)^{-1}\Sigma_k''(\omega)\Lambda_k'(\omega)$, which is of order T^4, and $(2S)^{-1}\Sigma_k'(\omega)\Lambda_k''(\omega)$, which is of order T^5. The third term vanishes except in the case that the imaginary part of the self-energy vanishes at the zero of the denominator, corresponding to an infinitely long-lived quasiparticle. It may thus be neglected, since at finite temperature the quasiparticles of the system always have a finite lifetime (except in the case $\omega=0$, which we do not treat).

To calculate the spectral weight function given by Eq. (18), we need to know both $\Sigma_k(\omega)$ and $\mathrm{Im}R_k(\omega)$. These functions will be obtained from the t matrix, which (according to Fig. 2) satisfies the following integral equation[26]:

$$t(k_1k_2q\omega)=V(k_1k_2q)+N^{-1}\sum_{k_3}\frac{V(k_3k_2q)\,t(k_1k_3q\omega)}{\omega-\epsilon_{q/2+k_3}-\epsilon_{q/2-k_3}+i\delta}, \tag{20}$$

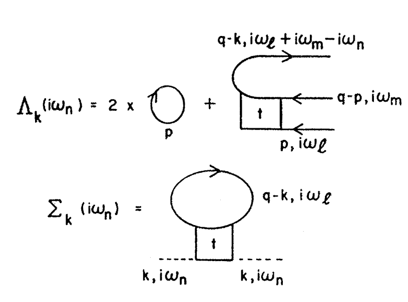

FIG. 3. The one-backward-line approximations for $\Lambda_k(i\omega_n)$ and $\Sigma_k(i\omega_n)$.

[23] R. Balian and C. DeDominicis, Nucl. Phys. **16**, 502 (1960).
[24] I. E. Dzyaloshinskii, Zh. Eksperim. i Teor. Fiz. **42**, 1126 (1962) [English transl.: Soviet Phys.—JETP **15**, 778 (1962)].
[25] G. Baym and A. M. Sessler, Phys. Rev. **131**, 2345 (1963).

[26] We have written the integral equation for the zero-temperature t matrix, neglecting $n_{q/2+k_3}+n_{q/2-k_3}$ in the numerator of the sum over k_3. This is consistent with the one-backward-line approximation, since the neglected terms are of the same order as the first two-backward-line diagram.

where

$$V(k_1k_2q)=-2J\sum_{\delta=x,y,z}\cos(\mathbf{k}_1\cdot\boldsymbol{\delta})\times[\cos(\mathbf{k}_2\cdot\boldsymbol{\delta})-\cos(\tfrac{1}{2}\mathbf{q}\cdot\boldsymbol{\delta})]. \quad (21)$$

The t matrix given by Eq. (20) is a function of both the relative incoming and outgoing momenta, $\mathbf{k}_1$ and $\mathbf{k}_2$, respectively, of the total momentum $\mathbf{q}$, and of the total energy ω carried by the two interacting spin waves. Equation (20) is very similar to equations discussed previously by Hanus,[27] Wortis,[8] and Boyd and Callaway,[10] and has the solution

$$t(k_1k_2q\omega)=-2J\sum_{\delta,\delta'=x,y,z}\{\cos(\mathbf{k}_1\cdot\boldsymbol{\delta})[\cos(\mathbf{k}_2\cdot\boldsymbol{\delta}')-\cos(\tfrac{1}{2}\mathbf{q}\cdot\boldsymbol{\delta}')][1-2\mathbf{A}(q,\omega)]_{\delta'\delta}{}^{-1}\}. \quad (22)$$

Here the matrix $\mathbf{A}$ is defined by

$$A_{ij}(\mathbf{q},\omega)=-\frac{J}{N}\sum_k\frac{\cos k_i(\cos k_j-\cos\frac{1}{2}q_j)}{\omega-\epsilon_{q/2+k}-\epsilon_{q/2-k}+i\delta} \quad (23a)$$

$$=-(1/4S)[D_{ij}(\mathbf{q},\tilde{\omega})-\alpha_jD_i(\mathbf{q},\tilde{\omega})], \quad (23b)$$

where

$$D_{ij}(\mathbf{k},x)=N^{-1}\sum_{k'}\frac{\cos k_i'\cos k_j'}{3(x-1)+\sum_m\alpha_m\cos k_m'+i\delta}, \quad (24a)$$

$$D_i(\mathbf{k},x)=N^{-1}\sum_{k'}\frac{\cos k_i'}{3(x-1)+\sum_m\alpha_m\cos k_m'+i\delta}, \quad (24b)$$

and below we will introduce also $D_0(\mathbf{k},x)$:

$$D_0(\mathbf{k},x)=N^{-1}\sum_{k'}[3(x-1)+\sum_m\alpha_m\cos k_m'+i\delta]^{-1}. \quad (24c)$$

Also we use the notation

$$\alpha_l=\cos\tfrac{1}{2}q_l, \quad (25a)$$

$$\tilde{\omega}=\omega/12JS. \quad (25b)$$

Note that $4SA_{ij}(\mathbf{q},\omega)$ is equal to $B_{ij}(\mathbf{q},\omega)$ as defined by Wortis. From Eq. (22) we see that the singularities of t are those of $(\mathbf{1}-2\mathbf{A})^{-1}$ and occur where

$$|\mathbf{1}-2\mathbf{A}(q,\omega)|=0.$$

It has been pointed out by the previous authors that these correspond to the two-spin-wave states, both the continuum of scattering states and the isolated two-particle bound states outside the continuum. More explicitly, the singularities of the t matrix are the following:

(1) In the limit $N^{-1}\sum_k\rightarrow(2\pi)^{-3}\int d^3k$, a continuum of poles, or a branch cut where the equation $\omega=\epsilon_{q/2+k}+\epsilon_{q/2-k}$ has a solution for some $\mathbf{k}$. This condition can also be written as

$$3(\tilde{\omega}-1)+\sum_m\alpha_m\cos k_m=0. \quad (26)$$

This represents the two-spin-wave band, which extends from

$$\omega_{\min}=4JS\sum_m(1-\alpha_m)$$

to

$$\omega_{\max}=4JS\sum_m(1+\alpha_m),$$

where $\mathbf{q}$ is the sum of the momenta of the two interacting spin-waves.

(2) Isolated poles below the continuum at the solutions of $|\mathbf{1}-2\mathbf{A}(\mathbf{q},\omega)|=0$, where the A_{ij} are real functions in this region. These are the bound states discussed in great detail by Wortis.[8] He found that a threshold exists for q, below which the bound states do not appear, and that the threshold goes to increasing q as the spin increases. In addition, he pointed out that there are at most three bound states. We will locate the bound states in agreement with the above and will also calculate the residue of t at the bound-state poles. From the above discussion and Eq. (20) it is clear that one may write a spectral representation for the t matrix

$$t(k_1k_2q\omega)=V(k_1k_2q)+\int_{-\infty}^{\infty}d\omega'\,\frac{B(k_1k_2q\omega')}{\omega'-\omega}, \quad (27)$$

where the spectral weight function B is real and is given by

$$B(k_1k_2q\omega)=(1/\pi)\,\mathrm{Im}t(k_1k_2q\omega). \quad (28)$$

The spectral weight function B is nonzero for ω' on the branch cut of t or at the poles of t corresponding to the bound states. We have plotted these regions of ω space versus k for $\mathbf{k}$ along the [111] direction in Fig. 4. Here $\mathbf{k}=k(1,1,1)$ and we have taken the lattice spacing to

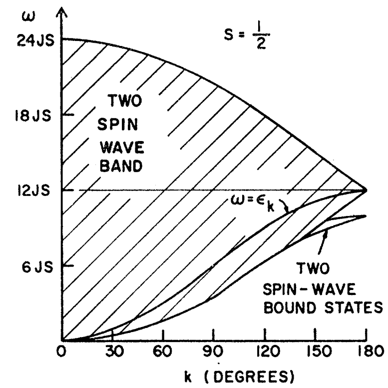

FIG. 4. The manifold of two-spin-wave states which determine the spectral weight function in the low-density approximation.

[27] J. Hanus, Phys. Rev. Letters 11, 336 (1963).

be unity, so that k is measured in degrees ("$k=d$ degrees" means $ka=d\pi/180$).

The diagrammatic equations in Fig. 3 enable us to write down expressions for $\Sigma_k(\omega)$ and $\Lambda_k(\omega)$ in terms of t. In the case $k_BT\ll\omega$,[28] where we may neglect the $n(\omega)$ terms in the frequency sums, we obtain, after performing these sums using the representation given by Eq. (27),

$$\Sigma_k(\omega)=\frac{1}{4\pi^3}\int d^3p\; n_p \times t[\tfrac{1}{2}(p-k),\tfrac{1}{2}(p-k),p+k,\omega+\epsilon_p], \quad (29a)$$

$$\Lambda_k(\omega)=\Lambda^{(1)}-\frac{1}{32\pi^6}\int d^3p\int d^3p' \times\frac{n_p t[p'-\frac{1}{2}(p+k),\frac{1}{2}(p-k),p+k,\omega+\epsilon_p]}{\omega+\epsilon_p-\epsilon_{p'}-\epsilon_{p+k-p'}+i\delta}. \quad (29b)$$

From Eq. (29) we may infer the analytic structure of $\Sigma_k(\omega)$ and $\Lambda_k(\omega)$ within our approximation. The factor n_p may be characterized as a sharply peaked function with a range in momentum space $\sim(k_BT/JS)^{1/2}$. Thus $\Sigma_k(\omega)$ and $\Lambda_k(\omega)$ will have appreciable spectral weight over essentially the same interval as the t matrix for total momentum $\mathbf{k}$. We may say that the spectral weight of $\Sigma_k(\omega)$ and $\Lambda_k(\omega)$ are obtained from that of the t matrix via a small thermal "smearing." Near the bound states the thermal smearing produces resonances in $\Sigma_k(\omega)$ and $\Lambda_k(\omega)$ from the poles in the t matrix.

As we have already noted, the one-backward-line approximation, Eq. (29), involves errors only of order T^5. However, in attempting to evaluate these expressions one runs into two difficulties. First, there is the problem of performing the three-dimensional momentum integrals. And then, since this must be done separately for each temperature, the evaluation and tabulation of the results becomes very unwieldy. In order to overcome these difficulties, we have decided to utilize the temperature expansion in our numerical work, and consider only the leading contributions which are of order $T^{5/2}$.[29]

To obtain the leading term in this expansion the $\mathbf{p}$ integrations in Eq. (29) may be performed in exactly the same manner as those encountered in the calculation of the thermodynamics of noninteracting spin waves, namely, the cofactor of n_p is expanded in powers of p. Thus we require an expansion of $[1-2\mathbf{A}(\mathbf{q},\omega)]^{-1}$ [see Eq. (22)] about $\mathbf{q}=\mathbf{k}$ in order to evaluate the integrals in Eq. (29). This expansion may be made except very near the Van Hove singularities of the t matrix or near the bound states, where the gradient of $[1-2\mathbf{A}(\mathbf{q},\omega)]^{-1}$ with respect to $\mathbf{q}$ becomes infinite. Thus the equations we are about to derive for $\Sigma_k(\omega)$ will not be valid in these regions. However, the Van Hove singularities affect the calculation of the spectral weight function only over a negligibly small region in ω space.[30] In the remaining region we use Eq. (22) for the t matrix and expand $[1-2\mathbf{A}(\mathbf{q},\omega)]^{-1}$ about $\mathbf{q}=\mathbf{k}$ and obtain, correct to order $T^{5/2}$,

$$\Sigma_k(\omega)=\frac{\Sigma^{(1)}(k)}{1-\gamma_k}\{\tfrac{2}{3}\sum_i(\sin^2\tfrac{1}{2}k_i)[1-2\mathbf{A}(\mathbf{k},\omega)]_{ii}^{-1}+\tfrac{4}{3}\sum_{i,j}(\sin\tfrac{1}{2}k_j)(\cos\tfrac{1}{2}k_i)(\partial/\partial k_j)[1-2\mathbf{A}(\mathbf{k},\omega)]_{ji}^{-1}\}. \quad (30)$$

Here $\Sigma^{(1)}(k)$ is the first Born approximation to $\Sigma_k(\omega)$, given by Eq. (29a) with t replaced by V:

$$\Sigma^{(1)}(k)=\frac{1}{4\pi^3}\int d^3p\; n_pV[\tfrac{1}{2}(p-k),\tfrac{1}{2}(p-k),p+k], \quad (31)$$

and is evaluated to order $T^{5/2}$ as

$$\Sigma^{(1)}(k)=-(\epsilon_k/32S)\zeta(\tfrac{5}{2})\pi^{-3/2}\tau^{5/2} \qquad (\tau=k_BT/JS). \quad (32)$$

It is possible to estimate the validity of this asymptotic evaluation of the low-density contribution by comparison with the asymptotic evaluation of a similar quantity,

$$n=(1/N)\sum_k\langle n_k\rangle_0=(1/N)\sum_k[\exp(\beta\epsilon_k)-1]^{-1}.$$

As has been pointed out,[31] this quantity can be expressed in closed form using modified Bessel functions. Thus one has available the complete asymptotic expansion of n at low temperatures. Although this expansion is not convergent (i.e., it is truly an asymptotic one), it can be seen that successive terms are smaller initially by a factor of $k_BT/4JS$. Thus one might anticipate that our expansions also have this property, or that the first neglected term is down by a factor $k_BT/4JS\equiv\frac{1}{4}\tau$.

The same procedure could in principle be used to evaluate $\Lambda_k(\omega)$ and thence, from Eq. (19), $R_k(\omega)$. However, since one obtains rather complicated expressions for $\Lambda_k(\omega)$, the following approach was found to be more convenient.

We define $\bar{R}_k(\omega)$ by

$$\bar{R}_k(\omega)=R_k(\omega)-\Sigma^{(1)}(k)-\left(\frac{\omega-\epsilon_k+i\delta}{2S}\right)\Lambda^{(1)}, \quad (33a)$$

$$\bar{R}_k(\omega)=[\Sigma_k(\omega)-\Sigma^{(1)}(k)]+\left(\frac{\omega-\epsilon_k+i\delta}{2S}\right)[\Lambda_k(\omega)-\Lambda^{(1)}]. \quad (33b)$$

[28] In the regime $k_BT\gg\omega$, in addition to keeping the neglected $n(\omega)$ term in Eq. (29a), one also must retain the terms $(1+n_{q/2+k_3}+n_{q/2-k_3})$ in Eq. (20) for the t matrix. This will be discussed more fully in a subsequent paper.

[29] In contrast to the approximation of taking only diagrams for $\Sigma_k(\omega)$ and $\Lambda_k(\omega)$ with one backward line, this approximation is not essential, and could be overcome at the cost of more intricate numerical evaluation.

[30] R. Silberglitt, Ph.D. thesis, University of Pennsylvania, 1968 (unpublished).

[31] T. Tanaka and S. J. Glass (unpublished), quoted by S. H. Charap and E. L. Boyd, Phys. Rev. 133, A811 (1964).

Note that since $\Sigma^{(1)}(k)$ and $\Lambda^{(1)}$ are real, one has that $\mathrm{Im}R_k(\omega)=\mathrm{Im}\bar{R}_k(\omega)$. Accordingly, to calculate $A_k(\omega)$ we may replace $R_k(\omega)$ in Eq. (18) by $\bar{R}_k(\omega)$. In Appendix B we derive the expression for $\bar{R}_k(\omega)$,

$$\bar{R}_k(\omega)=(1/S)(1/2\pi)^6\int d^3p\int d^3p'\,n_p\,\frac{t[p'-\frac{1}{2}(p+k),\frac{1}{2}(p-k),p+k,\omega+\epsilon_p]}{\omega+\epsilon_p-\epsilon_{p'}-\epsilon_{p+k-p'}+i\delta}\times(\epsilon_{k-p'}+\epsilon_{p-p'}-\epsilon_{p'}-\epsilon_{p+k-p'}). \quad (34)$$

This expression has the virtue that the cofactor of n_p is of order p^2 so that no gradients of $[1-2\mathbf{A}(\mathbf{k},\omega)]^{-1}$ are required for the calculation of the $T^{5/2}$ coefficient of $R_k(\omega)$. Using Eq. (22), we thus find

$$\bar{R}_k(\omega)=-[\Sigma^{(1)}(\pi)/3S]\sum_{i,j}(\sin^2\tfrac{1}{2}k_i)D_{ij}(\mathbf{k},\tilde{\omega})[1-2\mathbf{A}(\mathbf{k},\omega)]_{ji}^{-1}, \quad (35)$$

where $\Sigma^{(1)}(\pi)$ is $\Sigma^{(1)}(k)$ evaluated for $\mathbf{k}=(\pi,\pi,\pi)$.

Let us now consider the bound-state region. As is discussed by Hanus[27] and Wortis,[8] the bound states occur at the simple poles of $[1-2\mathbf{A}]^{-1}$. For $\mathbf{k}$ in the [111] direction the matrix A_{ij} has only two unique elements, $A_{ii}\equiv A_0$ and $A_{ij}\equiv A_0'$. In this case $(1-2\mathbf{A})^{-1}$ is readily found to be

$$(1-2\mathbf{A})^{-1}=\begin{pmatrix}1&1&1\\1&1&1\\1&1&1\end{pmatrix}\Big/3(1-2A_0-4A_0')+\begin{pmatrix}2&-1&-1\\-1&2&-1\\-1&-1&2\end{pmatrix}\Big/3(1-2A_0+2A_0'). \quad (36)$$

Thus, one sees that there is a symmetric or s-wave bound state[10] at ω_s given by

$$1-2A_0(k,\omega_s)-4A_0'(k,\omega_s)=0, \quad (37a)$$

and a doublet bound state which Boyd and Callaway[10] show is d-like at ω_D given by

$$1-2A_0(k,\omega_D)+2A_0'(k,\omega_D)=0. \quad (37b)$$

The calculation of the spectral weight function $A_k(\omega)$ in the vicinity of the bound states is extremely complicated. In view of the fact that the effect of thermal smearing is probably unimportant (this is consistent with our results) we will calculate the total area under the spectral weight function (total cross section) near the bound states. To do this we neglect thermal smearing, i.e., we make the pole approximation for $\Sigma_k(\omega)$ and $\Lambda_k(\omega)$, assuming them to be of the form

$$\Sigma_k(\omega)\sim\alpha_k/(\omega-\omega_B)+\beta_k+\gamma_k(\omega-\omega_B)+\cdots, \quad (38a)$$

$$\Lambda_k(\omega)\sim a_k/(\omega-\omega_B)+b_k+c_k(\omega-\omega_B)+\cdots, \quad (38b)$$

for ω near a bound state at ω_B. If one substitutes these three term expansions for $\Sigma_k(\omega)$ and $\Lambda_k(\omega)$ into Eq. (14), one finds a Green's function with two poles, one near ϵ_k and one near ω_B. To lowest order $(T^{5/2})$ the residue of the pole near ω_B is

$$2S(\omega_B-\epsilon_k)^{-2}[\alpha+(2S)^{-1}(\omega_B-\epsilon_k)a].$$

The factor in the square brackets is just the residue of $R_k(\omega)$ or $\bar{R}_k(\omega)$ at ω_B in the pole approximation. The pole approximation is generated from Eq. (34) by neglecting the dependence of the t matrix on ϵ_p, so that Eq. (35) is suitable for this purpose. Accordingly, using Eqs. (35) and (36), we find the total areas under the spectral weight function $a_k(\omega_s)$ and $a_k(\omega_D)$ near the

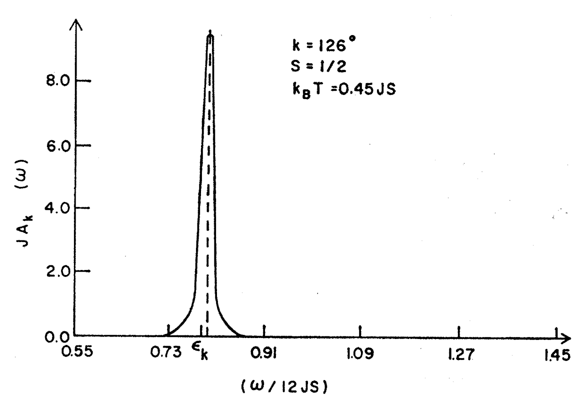

FIG. 5. The spectral weight function within the two-spin-wave band for $T\sim\frac{1}{4}T_c$.

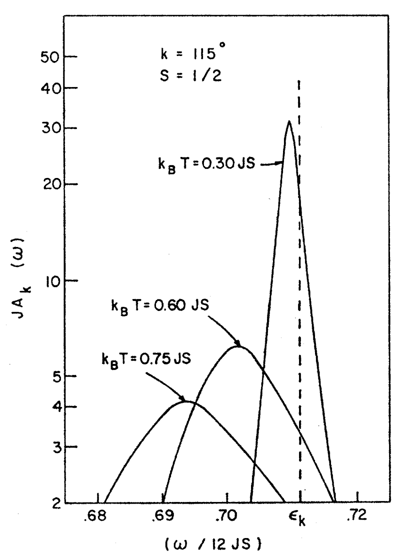

FIG. 6. The spectral weight function within the two-spin-wave band for $k<k_c$. Note the logarithmic scale for the ordinate.

bound states at ω_s and ω_D, respectively, to be

$$a_k(\omega_s)=\tfrac{2}{3}\Sigma^{(1)}(\pi)\,\frac{\sin^2\frac{1}{2}k}{(\omega_s-\epsilon_k)^2}\,\frac{D_{ii}(k,\tilde{\omega}_s)+2D_{ij}(k,\tilde{\omega}_s)}{[2(\partial/\partial\omega)A_0(k,\omega)+4(\partial/\partial\omega)A_0'(k,\omega)]|_{\omega_s}},\tag{39a}$$

$$a_k(\omega_D)=\tfrac{2}{3}\Sigma^{(1)}(\pi)\,\frac{\sin^2\frac{1}{2}k}{(\omega_D-\epsilon_k)^2}\,\frac{D_{ii}(k,\tilde{\omega}_D)-D_{ij}(k,\tilde{\omega}_D)}{[(\partial/\partial\omega)A_0(k,\omega)-(\partial/\partial\omega)A_0'(k,\omega)]|_{\omega_D}}.\tag{39b}$$

When one considers the point $\omega=\epsilon_k$, the sum rules[8] on $A_{ij}(\mathbf{k},\omega)$ and its derivatives simplify matters, and consequently, as is shown in Appendix C, a compact expression for the self-energy follows. It is the self-energy at $\omega=\epsilon_k$ that gives the renormalized spin-wave energy $\epsilon_k(T)$ and inverse lifetime or damping constant $\Gamma_k(T)$ through the relations

$$\epsilon_k(T)=\epsilon_k+\operatorname{Re}\Sigma_k(\epsilon_k),\tag{40a}$$

$$\Gamma_k(T)=-\operatorname{Im}\Sigma_k(\epsilon_k).\tag{40b}$$

The expression for $\Sigma_k(\epsilon_k)$ in the [111] direction was previously reported,[16] and is the following:

$$\Sigma_k(\epsilon_k)=Q(k)\Sigma^{(1)}(k),\tag{41a}$$

$$Q(k)=1+\frac{4A_0(k,\epsilon_k)}{1-3A_0(k,\epsilon_k)}-\frac{1}{3S}[1+3(\cos^2\tfrac{1}{2}k)D_0(k,\tilde{\epsilon}_k)].\tag{41b}$$

As we pointed out previously, Eq. (41) is the generalization to finite **k** of Dyson's Eq. (138) of his second paper.[7] The Dyson (long-wavelength) result has also been rederived within a Green's-function formalism by several authors.[13] We have generalized Eq. (41) to the $[11x]$ direction,[30] and the result is

$$\Sigma_k(\epsilon_k)=\tfrac{8}{3}\,\frac{\Sigma^{(1)}(k)}{1-\gamma_k}\,[F(k)+B^{(1)}(k)+B^{(2)}(k)],\tag{42}$$

with

$$F(k)=\tfrac{1}{4}\left\{\frac{\beta_x^2[(a+b+c-1)+b(a-c)]+\beta_z^2(a+c)(a-c)}{(a-c)(a+b+c-1)}\right\},\tag{43a}$$

$$B^{(1)}(k)=-(1/8S)(a+b+c-1)^{-1}\{2\beta_x^2\alpha_x(D_xb+[D_z(a+c-1)\alpha_x/\alpha_z])+\beta_z^2\alpha_z([D_x(b-1)\alpha_z/\alpha_x]+D_z(a+c))\},\tag{43b}$$

$$B^{(2)}(k)=-(1/8S)(a-c)^{-1}[\beta_x^2(D_{xx}-D_{xy})]-(1/8S)(a+b+c-1)^{-1}\{\beta_x^2\times[b(D_{xx}+D_{xy})+2(a+c-1)D_{xz}(\alpha_x/\alpha_z)]+\beta_z^2[(b-1)D_{xz}(\alpha_z/\alpha_x)+(a+c)D_{zz}]\},\tag{43c}$$

where we have used the definitions

$$a=1-2A_{xx},\qquad \alpha_i=\cos\tfrac{1}{2}k_i,$$
$$b=1-2A_{zz},\qquad \beta_i=\sin\tfrac{1}{2}k_i.\tag{44}$$
$$c=-2A_{xy},$$

The interpretation of Eqs. (41) and (42) is clear. Along the [111] direction the doublet bound state becomes a damped resonance within the two-spin-wave band. At $\omega=\epsilon_k$, the solution of Eq. (37b) becomes equivalent to the vanishing of the denominator of Eq. (41). Thus if the damped bound state may exist at or near $\omega=\epsilon_k$, corresponding to solution of the real part of Eq. (37b), it will cause a resonance in $\Sigma_k(\epsilon_k)$. When we generalize to the $[11x]$ direction, the doublet state is split, and thus we see two resonance denominators in Eq. (42). The sum rules on A_{ij} at $\omega=\epsilon_k$ cause the singlet condition (37a) never to be satisfied in this region, so that the singlet bound state never approaches the single spin-wave state and has no effect on $\Sigma_k(\epsilon_k)$. Physically the resonance may be viewed as follows. According to Eq. (29), the excitation energy of a spin wave is modified by continual collisions with long-wavelength spin waves. When the energy of the damped bound state crosses the single-particle energy, there is a resonance in the sense that the single spin wave can capture a thermal spin wave and form a damped bound state so that the two spin waves propagate as a pair during the lifetime of the damped bound state.

We close this section by noting the necessity of taking account of the difference between the spin and boson spectral weight functions, denoted by $A_k^S(\omega)$ and $A_k^B(\omega)$, respectively. As is well known, the stability of the system requires $\omega A_k^S(\omega)\geq 0$, whereas the boson spectral weight (due to the non-Hermiticity of $H_{\rm DM}$) does not have this property. For $\omega\approx\epsilon_k$ the difference between $A_k^S(\omega)$ and $A_k^B(\omega)$ is not very significant and theories that take account of this difference by the approximation

$$A_k^S(\omega)\approx-(\langle S^z\rangle/S)A_k^B(\omega)$$

will be qualitatively correct. However, in the vicinity of the bound states $A_k^B(\omega)$ changes sign, so that it is impossible to discuss the contribution of the bound states without a proper treatment of $\Lambda_k(\omega)$. In fact, one can show[30] that the inclusion of $\Lambda_k(\omega)$ as in Eq. (18) gives a spin spectral weight function that obeys the stability condition $\omega A_k(\omega)>0$. Furthermore, in order to calculate the static properties correctly to order T^4 as Dyson[7] has done, one must include $\Lambda_k(\omega)$, as is discussed in Appendix D. To our knowledge, we have displayed for the first time a Green's function for general spin capable of both a satisfactory dynamical description of spin waves and an evaluation of the thermodynamics to the same accuracy as Dyson's results.

IV. RESULTS OF THE CALCULATION

In order to perform the numerical calculations it is necessary to evaluate the matrix $A_{ij}(\mathbf{k},\omega)$. This was accomplished in two ways. Firstly, within the two-spin-wave band a Bessel function representation was used to reduce both real and imaginary parts of $A_{ij}(\mathbf{k},\omega)$ to sums of one-dimensional integrals over products of Bessel functions.[32–34] These integrals were performed through the use of polynomial approximations for the Bessel functions and a four-point Gaussian quadrature.[34] Secondly, outside the band all the A_{ij}'s are real and were written in terms of sums involving $(\gamma_k)^n$. These sums were evaluated to the same accuracy ($\sim$0.1%) as the integrals above, and the two methods were matched just outside the band (the integral method is valid for all ω, the summation method only outside the band). Since the spin enters our equations only as a scaling factor, all quantities may be evaluated with very little effort for any spin, i.e., the integrals which have been performed need only to be done once. These integrals have been tabulated[30] and can be used to calculate any of the following quantities for arbitrary spin. For convenience, in most cases we have made evaluations for spins of $\frac{1}{2}$, 1, $\frac{5}{2}$, sometimes for spins $\frac{1}{2}$ through $\frac{5}{2}$.

Since $\Sigma_k(\omega)$ and $\bar{R}_k(\omega)$ are proportional to $T^{5/2}$, it is easy to calculate the spectral weight function at any temperature. But we must remain within the range of validity of our approximation. The temperature expansion for dynamic quantities is derived from integrals with n_p factors just as are static quantities. As we have discussed in Sec. III, this strongly suggests that we have obtained asymptotic expansions for $\Sigma_k(\omega)$ and $\bar{R}_k(\omega)$ in the parameter $\frac{1}{4}\tau$ or $k_BT/4JS$. Thus

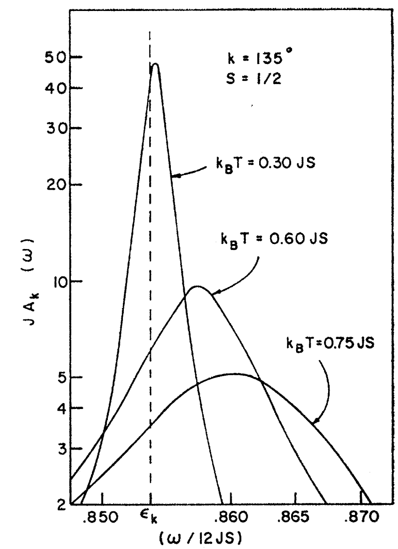

FIG. 7. The spectral weight function within the two-spin-wave band for $k>k_c$.

we anticipate that our calculation, which presumably neglects terms of order $(\frac{1}{4}\tau)^{7/2}$ in comparison with those of order $(\frac{1}{4}\tau)^{5/2}$, will be reliable for τ up to or near unity, the first neglected term being down by about a factor of 4 if $\tau=1$. From accurate theoretical expressions for the Curie temperature,[35] we see that $\tau=1$ corresponds to about $T=\frac{1}{2}T_c$ for spin $\frac{1}{2}$. Since it is believed that Dyson's result for the magnetization is valid up to about $\frac{1}{2}T_c$, our calculations should be valid in approximately the same temperature range, or for $0\leq\tau\lesssim1$. For these reasons we have chosen to evaluate the spectral weight function at various temperatures up to and including $\tau=1$.

The spectral weight function is plotted in the [111] direction (for spin $\frac{1}{2}$ and $k=126°$) versus ω within the two-spin-wave band in Fig. 5. The graph was obtained from numerical evaluation of Eqs. (18), (30), and (35) and the temperature chosen is near the middle of our range of validity, $k_BT=0.45JS$, or $T\approx\frac{1}{4}T_c$. Note the sharpness of the spectral weight even at this moderate temperature. This results from the fact that $\Sigma_k(\omega)$ is of order $T^{5/2}$, so that the factor $|\omega-\epsilon_k-\Sigma_k(\omega)|^{-2}$ in Eq. (18) has a very large value for ω within $T^{5/2}$ of ϵ_k, and is very small elsewhere. Due to the sharply peaked nature of $A_k(\omega)$, we must focus our attention on the region of ω space near ϵ_k in order to follow its temperature dependence. This is done in Figs. 6–8, where we plot $A_k(\omega)$ versus ω for various momenta, spins, and temperatures (the length of the abscissa in Fig. 6 is about $\frac{1}{20}$ of the continuum width). Again $\mathbf{k}$ is along the [111] direction. We observe many interesting effects in these graphs. First of all, as the temperature is increased, we see in all cases that the resonance broadens and moves further away from ϵ_k. We also find, as

[32] T. Wolfram and J. Callaway, Phys. Rev. **130**, 2207 (1963).
[33] M. Youssouff and J. Mahanty, Proc. Phys. Soc. (London) **85**, 1223 (1965).
[34] D. Hone, H. Callen, and L. R. Walker, Phys. Rev. **144**, 283 (1966).

[35] G. S. Rushbrooke and P. J. Wood, Mol. Phys. **1**, 257 (1958). A very crude rule of thumb is $(T/T_c)=3\tau/4(S+1)$.

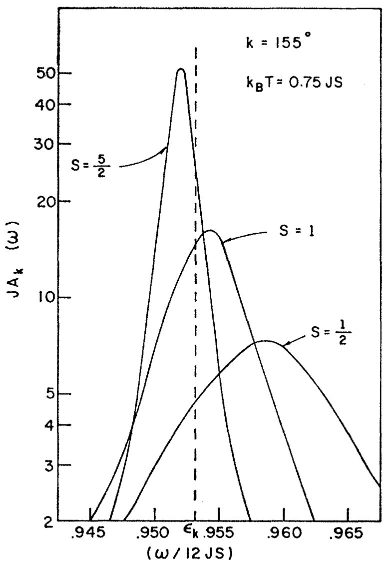

FIG. 8. The spectral weight function within the two-spin-wave band for various spins with $k>k_c(\frac{1}{2})$, $k_c(1)$ but $k<k_c(\frac{5}{2})$.

expected, that the resonance becomes sharper as the spin is increased. A striking result is that for k above some critical value (dependent on the spin), the renormalized energy is larger than the simple spin-wave energy. This phenomenon is due to the presence within the continuum of a new mode of the system, the damped bound state. This mode interacts with the single spin-wave state, causing a sign change in its renormalization and a sudden increase in its linewidth, both of which were anticipated from our Eqs. (41) and (42) for $\Sigma_k(\epsilon_k)$, which have a resonance structure. Our graphs of $\Sigma_k(\epsilon_k)$ from numerical evaluation of Eq. (41) (for **k** along the [111] direction) and (42) (for **k** along the [11x] direction) will display this resonance in $\Sigma_k(\omega)$ caused by the damped bound state.

The two spin-wave bound states will also have a significant effect on the magnon spectral weight function. To understand this, let us consider the solutions to the [111] bound-state equations, (37a) for the singlet and (37b) for the doublet. These solutions are plotted for spin $\frac{1}{2}$ in Fig. 9 and for spin 1 in Fig. 10. The solid lines represent solutions of Eqs. (37a) or (37b) outside the continuum, where both A_0 and A_0' are real and thus correspond to true bound states. The dotted lines represent solutions of the real part of Eq. (37b) within the continuum. Since the A's are complex in this region, the dotted line corresponds to a damped bound state, or a resonance rather than a pole in the t matrix. The amount of damping, which is determined by the magnitude of the imaginary part of $1-2A_0+2A_0'$, increases as the (doublet) state goes further into the continuum. The real part of Eq. (37a) has no solution within the continuum with small damping. Note that Figs. 9 and 10 display a very enlarged region of large momentum. This is done because there is a threshold

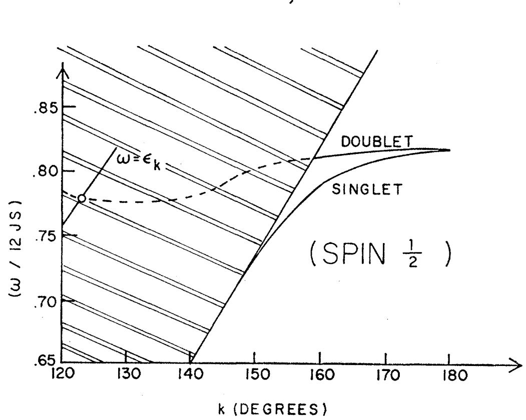

FIG. 9. The dispersion relations for the bound states for spin $\frac{1}{2}$ and $\mathbf{k}=k(1,1,1)$, showing the damped doublet state within the two-spin-wave band.

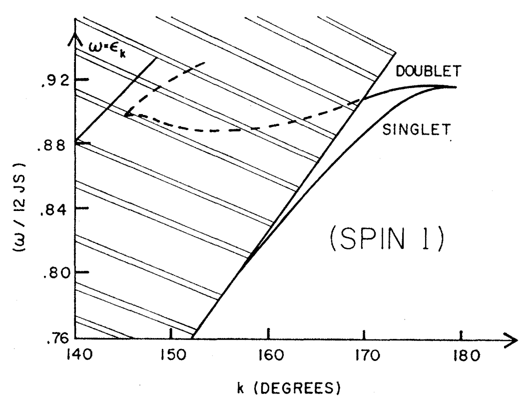

FIG. 10. The dispersion relations for the bound states for spin 1 and $\mathbf{k}=k(1,1,1)$, showing the damped doublet state within the two-spin-wave band.

($k=140°$ for spin $\frac{1}{2}$ and $k=157°$ for spin 1) below which no bound states appear, so that one seeks to examine carefully the upper region of the Brillouin zone. To place Figs. 9 and 10 in their proper perspective, compare with Fig. 4, which shows the whole Brillouin zone. Wortis[8] has demonstrated the existence of the two spin-wave bound states and plotted them outside the continuum, and Boyd and Callaway[10] have pointed out that the doublet state persists into the continuum. The new result shown by Figs. 9 and 10 is that the doublet state, although somewhat damped, goes far enough into the continuum so as to come very close to $\omega=\epsilon_k$ for spin 1 and to intersect it for spin $\frac{1}{2}$. This has the effect of introducing new energy states for the magnons with momentum near the region of close approach of the two modes (damped bound state and single spin-wave state). Thus the single magnon resonance will increase sharply in width, since the energy of a spin wave can be absorbed by the formation of a damped bound state in this region. The spin-wave energy shift will also be affected, changing sign because of the "repulsion" of the energy levels, much like one finds in simple perturbation theory.

If the temperature is very low, the spectral weight function in the neighborhood of the damped bound state is so small that this state is not observable as a bump in the curve. In this temperature regime there is only a tiny increase in the area under the spectral weight function near the damped bound state. However, even though this area increase is extremely small, it causes the main resonance to shift upward as we have observed in Figs. 7 and 8. The upward shift may be understood if one remembers that there is a sum rule on the first moment of $A_k(\omega)$ about $\omega=\epsilon_k$.[16,30] The contribution that a state makes to this first moment is not determined simply by its area, but by the area times its distance from ϵ_k. While at very low temperatures the amplitude of the spin-wave resonance may be orders of magnitude larger than that of the damped bound state, the latter is orders of magnitude farther from ϵ_k, so that both make comparable contributions to the first moment about ϵ_k. Thus the (small) increase in area (far from ϵ_k) because of the damped bound state is compensated by an upward shift of the spin-wave resonance, even at very low temperatures.

At higher temperatures one may actually observe the damped bound state as a resonance in $A_k(\omega)$, and its behavior in this regime is quite interesting. Let us focus our attention on the spectral weight function within the continuum for fixed spin and temperature, and follow the damped bound state as a function of momentum. We choose $k_BT=Js$ and spin $\frac{1}{2}$, so that $T\sim\frac{1}{2}T_c$. From Fig. 9 we see that the damped bound state should enter the continuum at about $k=140°$, continue inward as k is decreased, and coincide with the single spin-wave state at $k=124°$. In Fig. 11 we observe this phenomenon occurring. First, for $k=130°$ the bound state and single magnon state are both observable as resonances (shifted away from each other). They are coming closer together, with the main resonance increasing in width, when $k=125°$. Then at $k=124°$, which represents the intersection of the two modes, we observe two peaks of about equal height and width, so that one state cannot be distinguished from the other. As the momentum is decreased further, the bound state passes through the magnon state and then begins to lose its identity (as the damping increases). At this point the main resonance is also becoming sharper and has begun to shift downward, as it must. Finally, at $k=120°$ the bound state has been reduced to a slight shoulder in the spectral weight curve, and we are entering the region of momentum space where the bound states have no significant effect on the single spin-wave state.

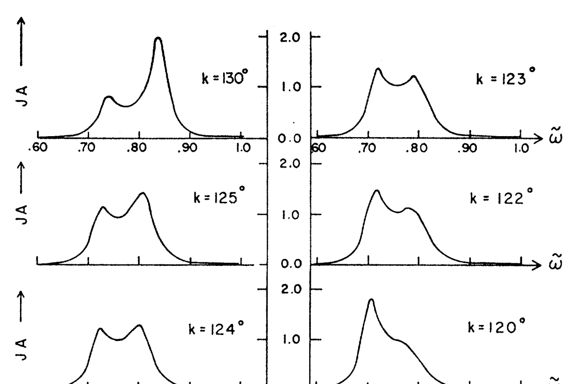

FIG. 11. The spectral weight function within the two-spin-wave band at $T\sim\frac{1}{2}T_c$ for spin $\frac{1}{2}$, showing the damped bound state resonance and the breakdown of the quasiparticle picture near $k=124°$, where the spin-wave mode and damped bound state mode intersect. Note that $\tilde{\omega}=\omega/12JS$.

As a check on the accuracy of our calculated spectral weight function, we have evaluated Eqs. (39a) and (39b) to obtain the area under the spectral weight at the true bound states and then numerically computed the first two moments of $A_k(\omega)$. Comparison of these numerical results with theoretical predictions from the sum rules has yielded excellent agreement. We shall display some results of these sum-rule checks in a moment, but first we make some comments on the sum rules themselves.

In our numerical calculations of the spectral weight function we have neglected terms in both the numerator and denominator of Eq. (16) of order higher than $\tau^{5/2}$. As we have remarked, this approximation was made for numerical convenience and is not essential. A more accurate treatment would thus replace $R_k''(\omega)$ in Eq. (18) by $R_k''(\omega)-(1/2S)\ \mathrm{Im}\Sigma_k^*(\omega)\Lambda_k(\omega)$. Among the neglected terms is the term $(1/2S)\Sigma_k''(\omega)\Lambda^{(1)}=-\Sigma_k''(\omega)(n/S)$. Inclusion of only this term would scale the spectral weight function by the factor $(1-n/S)=-\langle S^z\rangle/S$ near resonance. We have not included this factor for two reasons: (a) Its inclusion would be inconsistent in that other terms of comparable order should be included; (b) this term is actually frequency-dependent and would not lead to an everywhere positive spectral weight function. Thus, although our calculations give a reasonable evaluation[36] of Eq. (16), we should expect the sum rules to be satisfied only to lowest order in τ, in which case $\langle S^z\rangle=-S$. Defining $\tilde{\omega}=\omega/12JS$ and $\tilde{A}_k(\tilde{\omega})=JA_k(\tilde{\omega})$, the sum rules to lowest order in τ are[16,30]

$$M_0=\int_{-\infty}^{\infty}d\tilde{\omega}\,\tilde{A}_k(\tilde{\omega})=\tfrac{1}{6},\tag{45a}$$

$$M_1=\int_{-\infty}^{\infty}d\tilde{\omega}\,(\tilde{\omega}-\tilde{\epsilon}_k)\tilde{A}_k(\tilde{\omega})=\tfrac{1}{6}(12JS)^{-1}\Sigma^{(1)}(k)\tag{45b}$$

$$=-(\tilde{\epsilon}_k/12S)(1.51\times10^{-2})\tau^{5/2},\tag{45c}$$

where we have used Eq. (32) for $\Sigma^{(1)}(k)$. Some specific examples of the sum rule verifications are shown in

[36] In Appendix D we show that the thermodynamics as calculated using the spectral weight function of Eq. (16) are consistent with Dyson's results (Ref. 7).

Table I. Verification of the sum rules.[a]

k	S	T/T_c	M_0^{cont}	M_0^{sing}	M_0^{doub}	M_0^{calc}	M_0^{theor}	M_1^{cont}	M_1^{sing}	M_1^{doub}	M_1^{calc}	M_1^{theor}
115°	$\frac{1}{2}$	0.50	0.166	···	···	0.166	0.167	-0.171×10^{-2}	···	···	-0.171×10^{-2}	-0.179×10^{-2}
125°	$\frac{1}{2}$	0.50	0.169	···	···	0.169	0.167	-0.199×10^{-2}	···	···	-0.199×10^{-2}	-0.197×10^{-2}
135°	$\frac{1}{2}$	0.50	0.167	···	···	0.167	0.167	-0.214×10^{-2}	···	···	-0.214×10^{-2}	-0.219×10^{-2}
145°	$\frac{1}{2}$	0.38	0.1679	0.0005	···	0.168	0.167	-0.971×10^{-3}	-0.101×10^{-3}	···	-0.107×10^{-2}	-0.112×10^{-2}
170°	1	0.28	0.162	0.002	0.008	0.172	0.167	$+0.288\times10^{-3}$	-0.252×10^{-3}	-0.689×10^{-3}	-0.653×10^{-3}	-0.606×10^{-3}
160°	$\frac{1}{2}$	0.23	0.161	0.0008	0.0027	0.1645	0.167	$+0.240\times10^{-3}$	-0.152×10^{-3}	-0.418×10^{-3}	-0.330×10^{-3}	-0.329×10^{-3}
155°	1	0.23	0.167	···	···	0.167	0.167	-0.335×10^{-3}	···	···	-0.335×10^{-3}	-0.334×10^{-3}
126°	$\frac{5}{2}$	0.10	0.167	···	···	0.167	0.167	-0.540×10^{-4}	···	···	-0.540×10^{-4}	-0.541×10^{-4}

[a] The theoretical values are obtained from Eq. (45). The contributions to the moments from the continuum, the singlet bound state, and doublet bound state are denoted by the superscripts cont, sing, and doub, respectively. Also $\tau=\frac{4}{3}(S+1)T/T_c$.

Table I. The accuracy to which these sum rules are fulfilled assures us that the low-density approximation is a good one and that our numerical calculations are reliable. An important conclusion from Table I is that the amplitude of the spectral weight function at the bound states, i.e., M_0^{sing} and M_0^{doub}, is so small that their direct observation in the susceptibility seems to be a remote possibility. We see also from Table I that for small k ($k<k_c$) the contribution to M_1 from the continuum, M_1^{cont}, is negative, indicative of the fact that the main resonance occurs below ϵ_k due to renormalization. For $k>k_c$ the presence of a damped bound state within the continuum or of true bound states outside the continuum may push the main resonance above ϵ_k. In this case the positive contribution to M_1 from the single magnon state must be counterbalanced by the larger negative contribution from the bound states, so that M_1 is small and negative as required by Eq. (45c).

We have previously derived expressions for the self-energy at $\omega=\epsilon_k$, which gives the spin-wave renormalization and lifetimes through Eq. (40). In Figs. 12 and 13 we have plotted the real and imaginary parts of $\Sigma_k(\epsilon_k)$ in the [111] direction for spins $\frac{1}{2}$ and $\frac{3}{2}$, from numerical evaluation of Eq. (41). The dashed curve is $\Sigma^{(1)}(k)$, the first Born approximation. Note that, as we have pointed out previously, there is a resonance occurring in $\Sigma_k(\epsilon_k)$ in Eq. (41) as $\text{Re}A_0$ approaches $\frac{1}{3}$. This corresponds to the damped bound state which we have just discussed, $1-3A_0=0$ being the doublet equation at $\omega=\epsilon_k$. We find that at $\omega=\epsilon_k$ the singlet equation cannot be solved since $1-2A_0-4A_0'=1$. Thus only the doublet persists far enough into the continuum to

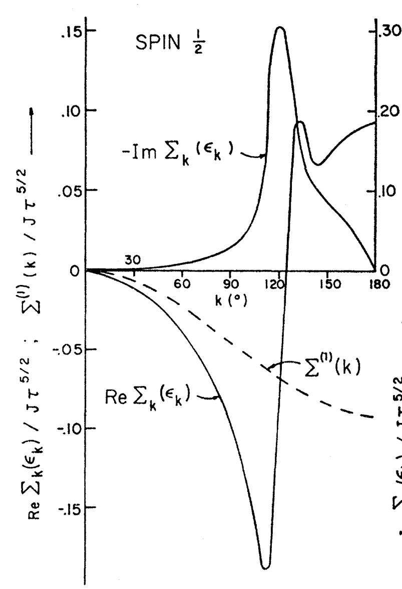

Fig. 12. The magnon self-energy at $\omega=\epsilon_k$ for spin $\frac{1}{2}$ and $\mathbf{k}=k(1,1,1)$, showing the resonance caused by the damped bound state. Here and in Figs. 13 and 14 k is measured in degrees.

affect the spin-wave energy shift and linewidth, as demonstrated also by Figs. 9 and 10. For spin $\frac{1}{2}$, the two modes coincide at $k=124°$ from Fig. 9.

We note at this point that the first Born approximation is quite poor except at very long wavelength.[37] At the zone edge $(k=\pi)$, $Q(\pi)=-\frac{1}{3}(1+1/S)$, which for spin $\frac{1}{2}$ is -1, the *negative* of the first Born result. In fact, since perturbation theory corresponds to expansion of $(1-3A_0)^{-1}$ in a geometric series, it converges only for $|3A_0|<1$. However, near resonance $\mathrm{Re}3A_0\sim 1$, and $\mathrm{Im}3A_0\neq 0$ since there is damping of the bound state. The damping will be reasonably large since the bound state has emerged quite far into the continuum, so that $|3A_0|$ will certainly surpass unity in the region near the resonance. For example, $|3A_0|=1$ at about $k=120°$ for spin $\frac{1}{2}$. Thus the resonance in the self-energy is a nonperturbative effect. We have obtained it only through inclusion of all orders in $1/S$ via the t matrix. As the spin is increased, one observes the resonance diminishing in magnitude and moving to larger momentum. This is as it must be, since for higher spin the bound states move further out toward the zone edge, finally vanishing in the limit of infinite spin.

In order to investigate the angular dependence of the spin-wave energy and lifetime, we have numerically evaluated Eq. (42) for $\Sigma_k(\epsilon_k)$ in the [11x] direction $(k_x=k_y\neq k_z)$. Figure 14 displays the results for $\mathbf{k}$ in the (11x) plane, at an angle of $\theta=9°$ from the [111] diagonal ($\theta=0°$ corresponds to [111], $\theta=36°$ corresponds to [110]). The plot is for spin $\frac{3}{2}$. The notable features are the following: There are now two peaks in $\Sigma_k''(\epsilon_k)$, corresponding to the two states of the (now nondegenerate) doublet. This double peaked behavior is observed for all spins except $\frac{1}{2}$. Comparison of Figs. 13 and 14 shows that the damped bound-state resonance is most prominent along the [111] direction. As one goes toward [110], the resonance decreases in magnitude and moves further out toward the zone edge. Thus we expect that the easiest place to experimentally observe the damped bound state will be along the [111] direction.

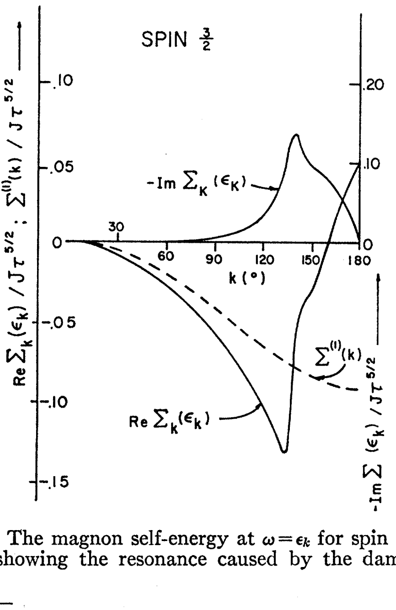

FIG. 13. The magnon self-energy at $\omega=\epsilon_k$ for spin $\frac{3}{2}$ and $\mathbf{k}=k$ (1, 1, 1), showing the resonance caused by the damped bound state.

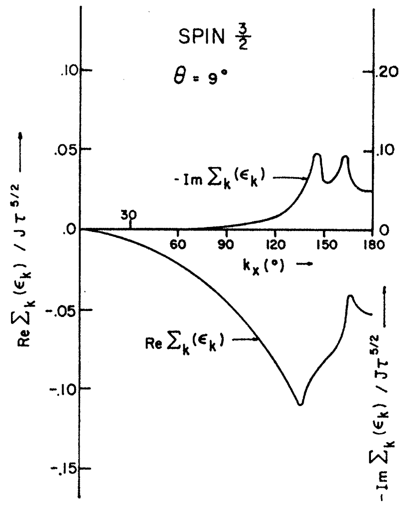

FIG. 14. The magnon self-energy at $\omega=\epsilon_k$ for spin $\frac{3}{2}$ and $\mathbf{k}=k_x$ (1, 1, k_z/k_x), showing the angular dependence of the resonance caused by the damped bound state.

V. CONCLUSIONS

The effect of the bound states on the main resonance is a specific example of a more general and familiar phenomenon. From general considerations it is clear that the emergence of a new mode or the proximity of two existing modes in a system will affect the single-particle spectral weight function. This is simply due to the noncrossing of energy levels in quantum mechanics. Other examples in many-body theory are the electron gas in the random phase approximation[38] (RPA) and the theory of spin fluctuations in nearly ferromagnetic metals.[12] In all three cases one may express the single-particle self-energy in terms of a function that has a pole reflecting some collective mode of the system (for us the t matrix and the two spin-wave bound states, in the RPA the inverse of the dielectric constant and the plasmons, for nearly ferromagnetic metals the particle-hole t matrix and the spin fluctuations or paramagnons). The renormalization and lifetimes of the quasiparticles of all these systems will thus show manifestations of the collective modes.

The analogy to the nearly ferromagnetic metal is particularly enlightening, and we will focus out attention on it. In the itinerant model of ferromagnetism,

[37] Remarkably, the first Born approximation for $\Sigma_k''(\epsilon_k)$ becomes exact as $k\to 0$. For $\epsilon_k\gg k_BT$ this was shown in Ref. 7. For $\epsilon_k\ll k_BT$ see A. B. Harris (to be published).

[38] D. Pines, *Elementary Excitations in Solids* (W. A. Benjamin, Inc., New York, 1963).

spin waves are viewed as bound electron-hole pairs,[39] and are manifest as poles in the particle-hole t matrix. Thus the *itinerant* spin waves are analogous to our two spin-wave bound states, which cause poles in our t matrix. In the case of a nearly ferromagnetic metal there are resonances (paramagnons or spin fluctuations) that affect the single-particle properties of the system. These paramagnons are the analog of our damped bound states, which appear as resonances in our t matrix, rather than poles (since they are inside the two spin-wave continuum). The transition from the damped bound state within the continuum to the true bound state outside is analogous to the transition from a nearly ferromagnetic to a ferromagnetic metal, or from paramagnons to true magnons. Thus we see that the electron mass enhancement caused by the spin fluctuations and the resonance in $\Sigma_k(\omega)$ caused by the damped bound state of two spin waves are two examples of the same phenomenon. In both cases, we have a system that in a certain regime is capable of supporting a collective mode. It then follows that near (but outside) this regime the fact that the collective mode can almost exist will have a significant influence on the single-particle properties of the system. In the near regime one says that a damped collective mode exists, which interacts with the single-particle excitations. Then the severity of the damping may be judged by the width of the corresponding resonance (which in the case of no damping would be a pole).

Our calculation of the spectral weight function at low temperatures has many important consequences:

(a) The area under the spectral weight function at the true bound states is so small that their direct observation *outside* the two-spin-wave band is a very remote possibility.

(b) At very low temperatures (perhaps $T \lesssim 0.2T_c$), or far away from the damped bound-state region, the spin-wave energy shift and linewidth are given very accurately by the real and imaginary parts of the self-energy evaluated at resonance, thus verifying the quasi-particle nature of the system.

(c) The presence of the spin-wave bound states (both true and damped) intimately affects the magnon renormalization and lifetime. In addition there is a region of close proximity of the spin wave and damped bound-state modes, within which the quasiparticle approximation breaks down.

(d) The damped bound state is observable both indirectly, through the resonance it causes in the magnon self-energy, and directly, at least within our approximation, as a resonance in the spin-wave spectral weight function (which gives the neutron scattering cross section).

In this work, we have treated for mathematical convenience a simple cubic magnet, and have neglected anisotropy and dipolar interactions. The generalization to more complicated cubic lattices is straightforward and not very difficult, merely introducing some numerical geometric factors. The inclusion of an anisotropy term of the form βS_z^2, where $\beta \ll J$, also presents no particular problem, since the extra terms in $\mathcal{H}_{DM}$ are of the same form as those already treated. To include dipolar interactions would be harder, since one would first have to transform to a representation that diagonalizes the dipolar interaction,[3] and this would change the nature of the diagrammatic series for the Green's function.

[39] T. Izuyama, D. Kim, and R. Kubo, J. Phys. Soc. Japan 18, 1025 (1963).

ACKNOWLEDGMENT

The authors would like to thank Professor D. Hone for helpful advice on the calculation of $A_{ij}(\mathbf{k}, \omega)$.

APPENDIX A: JUSTIFICATION OF NEGLECT OF KINEMATICAL INTERACTION

In the body of this paper, we have utilized Dyson's proof that the kinematical interaction contributes nothing to the low-temperature expansions which we have employed; i.e., the contribution of the nonphysical states to the thermodynamic traces considered is always of the form $e^{-\beta\Delta}$ and can thus be neglected in the temperature regime under consideration. Although Dyson's proof was conceived for static quantities, the generalization to the dynamic case is straightforward. The proof, which is given in Secs. 3 and 4 of his second paper,[7] is accomplished through a demonstration that there is a finite energy gap Δ between the lowest physical and the lowest nonphysical eigenstates of $\mathcal{H}_{DM}$. Thus the contribution of a nonphysical state to the partition function is smaller than that of a physical state by the factor $e^{-\beta\Delta}$. It then follows (unless the partition sum itself diverges) that to any finite order in the temperature the full partition function is equal to that obtained by summing only over the physical states. To prove a similar theorem for the spin-wave Green's function, we note two facts.

(a) We are always concerned with thermodynamic traces, quantities of the form

$$\sum_n (\exp-\beta E_n)\langle n \mid 0(S^+, S^-, S^z) \mid n\rangle.$$

(b) Matrix elements of any operator $O\,(S^+, S^-, S^z)$ from physical to nonphysical states vanish in the DM representation, since $S^+=(2S)^{1/2}a^+(1-n/2S)$, so that $S^+ \mid n\rangle=0$ if $n=2S$.

From (a) and (b) we see that we may always separate a trace into a proper and an improper part, the former from physical states and the latter from nonphysical states. Since a trace is a sum of *diagonal* matrix elements, there is no interference between the physical and nonphysical subspaces, for one would have to allow matrix elements both into and out of the nonphysical space for this to occur. Now we have, for any operator O, $\mathrm{tr}\rho O=(\mathrm{tr}\rho O)_P+(\mathrm{tr}\rho O)_I$, and the improper trace is of order $e^{-\beta\Delta}$ by Dyson's argument, since each term in it has the factor $\exp(-\beta E_n)$, where $|\psi_n\rangle$ is a nonphysical eigenstate. Thus we find to any finite order in the temperature that any of the dynamical quantities we discuss in this paper may be calculated by summing over all states. The results thus obtained are identical to those that would be obtained by restricting the sum to the physical subspace.

APPENDIX B: DERIVATION OF THE EXPRESSION FOR $\bar{R}_k(\omega)$

The definition, Eq. (30b), gives $\bar{R}_k(\omega)$ in terms of $\Sigma_k(\omega)-\Sigma^{(1)}(k)$ and $\Lambda_k(\omega)-\Lambda^{(1)}$. These functions are given by Eq. (29) as

$$\Sigma_k(\omega)-\Sigma^{(1)}(k)=\frac{1}{4\pi^3}\int d^3p\, n_p \times\{t[\tfrac{1}{2}(p-k),\tfrac{1}{2}(p-k),p+k,\omega+\epsilon_p] -V[\tfrac{1}{2}(p-k),\tfrac{1}{2}(p-k),p+k]\}, \quad \text{(B1)}$$

$$\Lambda_k(\omega)-\Lambda^{(1)}=-\frac{1}{32\pi^6}\int d^3p\int d^3p'\, n_p \times\frac{t[p'-\frac{1}{2}(p+k),\frac{1}{2}(p-k),p+k,\omega+\epsilon_p]}{\omega+\epsilon_p-\epsilon_{p'}-\epsilon_{p+k-p'}+i\delta}. \quad \text{(B2)}$$

From the t-matrix equation, Eq. (20), we see that $t-V=VGGt$. Substituting this into Eq. (B1), and writing the V's in terms of magnon energies, we find that

$$\Sigma_k(\omega)-\Sigma^{(1)}(k)=\frac{1}{4\pi^3}\int d^3p\, n_p(1/2\pi)^3\int d^3p'\frac{(1/2S)(\epsilon_{k-p'}+\epsilon_{p-p'}-\epsilon_k-\epsilon_p)}{\omega+\epsilon_p-\epsilon_{p'}-\epsilon_{p+k-p'}+i\delta}\, t[p'-\tfrac{1}{2}(p+k),\tfrac{1}{2}(p-k),p+k,\omega+\epsilon_p]. \quad \text{(B3)}$$

Multiplying Eq. (B2) by $(\omega-\epsilon_k+i\delta)/2S$ and adding the result to Eq. (B3), we obtain

$$\bar{R}_k(\omega)=\Sigma_k(\omega)-\Sigma^{(1)}(k)+\left(\frac{\omega-\epsilon_k+i\delta}{2S}\right)(\Lambda_k(\omega)-\Lambda^{(1)})$$
$$=\frac{1}{32\pi^6}\int d^3p\int d^3p'\, n_p\frac{t[p'-\frac{1}{2}(p+k),\frac{1}{2}(p-k),p+k,\omega+\epsilon_p]}{\omega+\epsilon_p-\epsilon_{p'}-\epsilon_{p+k-p'}+i\delta}\times F(p,p',k,\omega), \quad \text{(B4)}$$

where

$$F(p,p',k,\omega)=(1/2S)(\epsilon_{k-p'}+\epsilon_{p-p'}-\epsilon_p-\omega-i\delta); \quad \text{(B5)}$$

making the separation

$$\frac{2SF(p,p',k,\omega)}{\omega+\epsilon_p-\epsilon_{p'}-\epsilon_{p+k-p'}+i\delta}=-1+\frac{\epsilon_{k-p'}+\epsilon_{p-p'}-\epsilon_{p'}-\epsilon_{p+k-p'}}{\omega+\epsilon_p-\epsilon_{p'}-\epsilon_{p+k-p'}+i\delta}, \quad \text{(B6)}$$

and noting that the unity term vanishes when the $\mathbf{P}'$ integral in (B4) is performed, we obtain finally

$$\bar{R}_k(\omega)=\frac{1}{32\pi^6}\int d^3p\int d^3p'\, n_p\frac{t[p'-\frac{1}{2}(p+k),\frac{1}{2}(p-k),p+k,\omega+\epsilon_p]}{\omega+\epsilon_p-\epsilon_{p'}-\epsilon_{p+k-p'}+i\delta}\times(\epsilon_{k-p'}+\epsilon_{p-p'}-\epsilon_{p'}-\epsilon_{p+k-p'}), \quad \text{(B7)}$$

which is the desired result.

APPENDIX C: EVALUATION OF $\Sigma_k(\epsilon_k)$

In this Appendix we will exploit the simplifications that occur in the expression for $\Sigma_k(\omega)$ when $\omega=\epsilon_k$. From Eq. (30) we have

$$\Sigma_k(\omega)=\Sigma^{(1)}(k)[1-\gamma_k]^{-1} \times\{\tfrac{2}{3}\sum_i\beta_i^2[1-2\mathbf{A}(\mathbf{k},\omega)]_{ii}^{-1}+\tfrac{4}{3}\sum_{ij}\alpha_i\beta_j(\partial/\partial k_j) \times[1-2\mathbf{A}(\mathbf{k},\omega)]_{ji}^{-1}\}, \quad \text{(C1)}$$

where $\alpha_i=\cos\frac{1}{2}k_i$ and $\beta_i=\sin\frac{1}{2}k_i$. To compute the derivative we use the matrix relation

$$\partial\mathbf{M}^{-1}/\partial x=-\mathbf{M}^{-1}(\partial\mathbf{M}/\partial x)\mathbf{M}^{-1}. \quad \text{(C2)}$$

If we denote the second term inside the brackets of Eq. (C1) by T, we have

$$T=\tfrac{8}{3}\sum_{ijlm}\alpha_i\beta_j[1-2\mathbf{A}(\mathbf{k},\omega)]_{jl}^{-1} \times(\partial/\partial k_j)A_{lm}(\mathbf{k},\omega)[1-2\mathbf{A}(\mathbf{k},\omega)]_{mi}^{-1}. \quad \text{(C3)}$$

In order to simplify this expression we will use the sum rules[8] in the D_i and D_{ij} for the special case $\omega=\epsilon_k$;

$$\sum_i\alpha_iD_{ij}=\sum_i\alpha_iD_{ji}=D_j\sum_i\alpha_i^2, \quad \text{(C4a)}$$

$$\sum_j\alpha_iD_i=1+D_0\sum_i\alpha_i^2, \quad \text{(C4b)}$$

$$\sum_j\alpha_jD_{ij}{}^l=D_{il}+D_i{}^l\sum_i\alpha_i^2. \quad \text{(C4c)}$$

Here the D functions were defined in Eq. (24) with the exception of

$$D_i^j(\mathbf{k}, x) \equiv -(\partial/\partial\alpha_j) D_i(\mathbf{k}, x) \tag{C5a}$$

$$= N^{-1} \sum_\lambda \frac{\cos\lambda_i \cos\lambda_j}{[3(x-1)+ \sum_m \alpha_m \cos\lambda_m + i\delta]^2} \tag{C5b}$$

and

$$D_{ij}^l(\mathbf{k}, x) \equiv -(\partial/\partial\alpha_l) D_{ij}(\mathbf{k}, x) \tag{C5c}$$

$$= N^{-1} \sum_\lambda \frac{\cos\lambda_i \cos\lambda_j \cos\lambda_l}{[3(x-1)+ \sum_m \alpha_m \cos\lambda_m + i\delta]^2}. \tag{C5d}$$

We consider $\partial A_{lm}(\mathbf{k}, \omega)/\partial k_j$.

$$\partial A_{lm}(\mathbf{k}, \omega)/\partial k_j = -\tfrac{1}{2}\beta_j \partial A_{lm}(\mathbf{k}, \omega)/\partial\alpha_j \tag{C6a}$$

$$= (\beta_j/8S)(\partial/\partial\alpha_j)[D_{lm}(\mathbf{k}, \tilde{\omega}) - D_l(\mathbf{k}, \tilde{\omega})\alpha_m] \tag{C6b}$$

$$= -(\beta_j/8S)[D_{lm}^j(\mathbf{k}, \tilde{\omega}) - D_l^j(\mathbf{k}, \tilde{\omega})\alpha_m + \delta_{mj} D_l(\mathbf{k}, \tilde{\omega})], \tag{C6c}$$

where we have used Eqs. (23b) and (C5). Thus we find

$$T = -\frac{1}{3S} \sum_{ijlm} \alpha_i \beta_j^2 [1-2\mathbf{A}(\mathbf{k}, \epsilon_k)^{-1}]_{jl} [D_{lm}^j(\mathbf{k}, \tilde{\epsilon}_k) - \alpha_m D_l^j(\mathbf{k}, \tilde{\epsilon}_k) + \delta_{mj} D_l(\mathbf{k}, \tilde{\epsilon}_k)][1-2\mathbf{A}(\mathbf{k}, \epsilon_k)]_{mi}^{-1}. \tag{C7}$$

Note that

$$\sum_i [1-2\mathbf{A}(\mathbf{k}, \epsilon_k)]_{mi} \alpha_i^{-1} = \sum_i \{\delta_{mi} + [(1-2\mathbf{A}(\mathbf{k}, \epsilon_k))^{-1} 2\mathbf{A}(\mathbf{k}, \epsilon_k)]_{mi}\} \alpha_i \tag{C8a}$$

$$= \alpha_m + 2 \sum_{in} [1-2\mathbf{A}(\mathbf{k}, \epsilon_k)]_{mn}^{-1} \mathbf{A}(\mathbf{k}, \epsilon_k)_{ni} \alpha_i \tag{C8b}$$

$$= \alpha_m - (2S)^{-1} \sum_{in} [1-2\mathbf{A}(\mathbf{k}, \epsilon_k)]_{mn}^{-1} [D_{ni}(\mathbf{k}, \tilde{\epsilon}_k) - \alpha_i D_n(\mathbf{k}, \tilde{\epsilon}_k)] \alpha_i \tag{C8c}$$

$$= \alpha_m. \tag{C8d}$$

Here Eq. (C8a) is a matrix identity, and we have used Eq. (23b); to get Eq. (C8d) we have used Eq. (C4a). Thus Eq. (C7) becomes

$$T = -\frac{1}{3S} \sum_{jlm} \alpha_m \beta_j^2 [1-2\mathbf{A}(\mathbf{k}, \epsilon_k)]_{jl}^{-1} [D_{lm}^j(\mathbf{k}, \tilde{\epsilon}_k) - \alpha_m D_l^j(\mathbf{k}, \tilde{\epsilon}_k) + \delta_{mj} D_l(\mathbf{k}, \tilde{\epsilon}_k)] \tag{C9a}$$

$$= -\frac{1}{3S} \sum_{jl} \beta_j^2 [1-2\mathbf{A}(\mathbf{k}, \epsilon_k)]_{jl}^{-1} \times [D_{lj}(\mathbf{k}, \tilde{\epsilon}_k) + \alpha_j D_l(\mathbf{k}, \tilde{\epsilon}_k)], \tag{C9b}$$

where we have used Eq. (C4c). Furthermore, by Eq. (23b) this may be written as

$$T = -\frac{1}{3S} \sum_{jl} \beta_j^2 [1-2\mathbf{A}(\mathbf{k}, \tilde{\epsilon}_k)]_{jl}^{-1} \times [-4SA_{lj}(\mathbf{k}, \epsilon_k) + 2\alpha_j D_l(\mathbf{k}, \tilde{\epsilon}_k)] \tag{C10a}$$

$$= -\tfrac{2}{3} \sum_j \beta_j^2 + \tfrac{2}{3} \sum_j \beta_j^2 [1-2\mathbf{A}(\mathbf{k}, \epsilon_k)]_{jj}^{-1} - \frac{2}{3S} \sum_{jl} \beta_j^2 \alpha_j [1-2\mathbf{A}(\mathbf{k}, \epsilon_k)]_{jl}^{-1} D_l(\mathbf{k}, \tilde{\epsilon}_k). \tag{C10b}$$

Substituting this result into Eq. (C1), we thus find

$$\Sigma_k(\epsilon_k) = \Sigma^{(1)}(k)[1-\gamma_k]^{-1} \{\tfrac{2}{3} \sum_j \beta_j^2 - (2/3S) \sum_{jl} \beta_j^2 [1-2\mathbf{A}(\mathbf{k}, \epsilon_k)]_{jl}^{-1} D_{lj}(\mathbf{k}, \tilde{\epsilon}_k)\}. \tag{C11}$$

For $\mathbf{k} = k(111)$ this simplifies further through the use of Eq. (36), so that one obtains $Q(\mathbf{k})$ as given in the text.

APPENDIX D: STATIC CORRELATION FUNCTION

We may calculate the static correlation function $\langle S_k^+ S_k^- \rangle$ from the spectral weight function as

$$\langle S_k^+ S_k^- \rangle = \int_{-\infty}^{\infty} d\omega\, A_k(\omega) n(\omega). \tag{D1}$$

In order to compare our results with those previously obtained by other authors we will consider $\langle S_i^+ S_i^- \rangle$:

$$\langle S_i^+ S_i^- \rangle = N^{-1} \sum_k \langle S_k^+ S_k^- \rangle \equiv 2SC. \tag{D2}$$

Wortis[40] has calculated this quantity using a *static spin*

[40] M. Wortis, Ph.D. thesis, Harvard University, 1962 (unpublished).

formalism and finds

$$(1/2S)\langle S_i^+S_i^-\rangle = n_0 - 2n_0^2(1-1/2S) + [Q(0)/\pi S]\zeta(\tfrac{5}{2})\zeta(\tfrac{3}{2})(k_BT/4JS)^4, \quad \text{(D3)}$$

where n_0 is the unperturbed value of the number of spin-wave excitations. Note that the spin kinematics manifests itself by the term $-2n_0^2(1-1/2S)$ which for $S>\frac{1}{2}$ is of order T^3. Wortis also showed that this result was consistent with Dyson's[7] thermodynamics. The point that we wish to check is that our spin-spectral weight function gives a correct evaluation of $\langle S_i^+S_i^-\rangle$.

We use Eq. (16) for $A_k(\omega)$ and will approximate $\Lambda_k(\omega)$ and $\Sigma_k(\omega)$ by their one-backward-line expressions. Although we were able to approximate $A_k(\omega)$ using Eq. (18) for the dynamical properties, it is necessary to use Eq. (16) for the static properties. Strictly speaking, therefore, the dynamical spectral weight function that

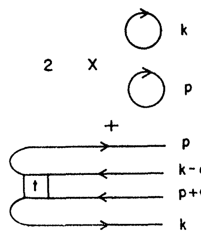

FIG. 15. Diagrams contributing to the spin correlation function of Eq. (D2).

we have evaluated will not reproduce Wortis's results. However, as mentioned before, the approximation of Eq. (18) in dropping some of the terms was simply one of numerical convenience. In principle there is no difficulty in using Eq. (16) for the dynamics. Accordingly we feel justified in claiming that Eq. (16), when evaluated using the one-backward-line approximation for $\Sigma_k(\omega)$ and $\Lambda_k(\omega)$, does give consistently both the static and dynamic properties of the Heisenberg ferromagnet. The one missing step in the argument then is to show that Eq. (D3) follows from Eq. (16).

We note that direct integration of $A_k(\omega)$ is difficult, but

$$C=\frac{1}{2NS}\sum_k\int_{-\infty}^{\infty}d\omega\, A_k{}^S(\omega)n(\omega)$$

$$=-\frac{1}{2NS\beta}\sum_{k,\omega_n}\mathcal{G}_k{}^S(i\omega_n)\exp(-i\omega_n\tau)\,|_{\tau=0-}, \quad \text{(D4a)}$$

where

$$(1/2S)\mathcal{G}_k{}^S(i\omega_n)=[1+(1/2S)\Lambda_k(i\omega_n)] \times[i\omega_n-\epsilon_k-\Sigma_k(i\omega_n)]^{-1}. \quad \text{(D4b)}$$

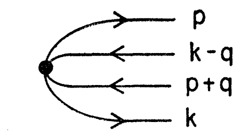

FIG. 16. Leading contribution to second term of Fig. 15.

Thus, denoting $\mathcal{G}^0(k,i\omega_n)\equiv(i\omega_n-\epsilon_k)^{-1}$,

$$C=-\frac{1}{N\beta}\sum_{k,\omega_n}[1+(1/2S)\Lambda_k(i\omega_n)] [\mathcal{G}^0(k,i\omega_n)+\mathcal{G}^0(k,i\omega_n)\Sigma_k(i\omega_n)\mathcal{G}^0(k,i\omega_n)+\cdots] \times\exp(i\omega_n0^+), \quad \text{(D5)}$$

which is justified by the uniform (in both k and ω_n) convergence of the series since $|\Sigma_k(i\omega_n)/\epsilon_k|\ll 1$. The neglected terms are of order T^5 at least. Therefore

$$C=-\frac{1}{N\beta}\sum_{k,\omega_n}\{\mathcal{G}^0(k,i\omega_n)+\Sigma_k(i\omega_n)[\mathcal{G}^0(k,i\omega_n)]^2 +(1/2S)\mathcal{G}^0(k,i\omega_n)\Lambda_k(i\omega_n)+(1/2S)[\mathcal{G}^0(k,i\omega_n)]^2 \times\Lambda_k(i\omega_n)\Sigma_k(i\omega_n)\}. \quad \text{(D6)}$$

The last term contains the factors $T^{3/2}$ from $\Lambda_k(i\omega_n)$ and $T^{5/2}$ from $\Sigma_k(i\omega_n)$ and also the sum over $i\omega_n$ introduces a factor $T^{3/2}$. Also, as is well known, the first two terms give the Dyson result for the number of excitations,

$$-\frac{1}{N\beta}\sum_{k,\omega_n}\mathcal{G}^0(k,i\omega_n)[1+\Sigma_k(i\omega_n)\mathcal{G}^0(k,i\omega_n)] =n^0+[Q(0)/\pi S]\zeta(\tfrac{5}{2})\zeta(\tfrac{3}{2})(k_BT/4JS)^4. \quad \text{(D7)}$$

We now evaluate

$$-\frac{1}{2N\beta S}\sum_{k,\omega_n}\Lambda_k(i\omega_n)\mathcal{G}^0(k,i\omega_n)$$

from the diagrams shown in Fig. 15. The first diagram gives just

$$-\frac{2}{N^2}\sum_{k,p}n_kn_p=-2n_0^2. \quad \text{(D8)}$$

We will show below that the full contribution of the

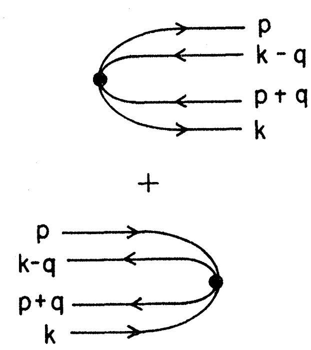

FIG. 17. Diagrams corresponding to Fig. 16 in backward-line formalism.

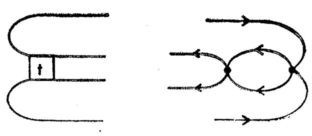

(a) (b)

FIG. 18. Higher-order contributions to the correlation function.

second diagram to order T^4 is obtained only from the diagram corresponding to $t=V$. For now, let us examine this diagram, given in Fig. 16. Its contribution is

$$\frac{2}{\beta^3}\sum_{\omega_m,\omega_l,\omega_n}\frac{1}{N^3}\sum_{pqk}\frac{V[q+\frac{1}{2}(p-k),\ \frac{1}{2}(p-k),\ p+k]}{(i\omega_n-\epsilon_k)(i\omega_l-\epsilon_{p+q})(i\omega_m-\epsilon_{k-q})}\times(i\omega_m+i\omega_l-i\omega_n-\epsilon_p)^{-1}.$$

Instead of explicitly performing the frequency sums, we note that the result must just be equal to the sum of the contributions of all the corresponding diagrams drawn in the Baym-Sessler formalism[25] which we have discussed in Sec. III. These contributions are found by including a factor of n_k for each backward line of momentum $\mathbf{k}$, $1+n_k$ for each forward line of momentum $\mathbf{k}$, and energy denominators consisting of

$$[\sum_{k_i}(\epsilon_{k_i})_{\text{for}}-\sum_{k_i}(\epsilon_{k_i})_{\text{back}}]^{-1}.$$

Corresponding to the above diagram, there are two diagrams in the new formalism, shown in Fig. 17, and giving contributions[41]

$$-\frac{2}{N^3}\sum_{pkq}\frac{n_pn_kV[q+\frac{1}{2}(p-k),\ \frac{1}{2}(p-k),\ p+k]}{\epsilon_k+\epsilon_p-\epsilon_{k-q}-\epsilon_{p+q}} \qquad \text{(D9a)}$$

and

$$\frac{2}{N^3}\sum_{pkq}\frac{n_pn_kV[\frac{1}{2}(p-k),\ q+\frac{1}{2}(p-k),\ p+k]}{\epsilon_k+\epsilon_p-\epsilon_{k-q}-\epsilon_{p+q}}. \qquad \text{(D9b)}$$

Now we know that

$$V(k_1k_2q)=-2J\times\sum_{\delta=x,y,z}\cos(\mathbf{k}_1\cdot\boldsymbol{\delta})[\cos(\mathbf{k}_2\cdot\boldsymbol{\delta})-\cos(\tfrac{1}{2}\mathbf{q}\cdot\boldsymbol{\delta})], \qquad \text{(D10)}$$

so that $V[q+\frac{1}{2}(p-k),\ \frac{1}{2}(p-k),\ p+k]$ contributes a factor $\sin(\frac{1}{2}\mathbf{k}\cdot\boldsymbol{\delta})\ \sin(\frac{1}{2}\mathbf{p}\cdot\boldsymbol{\delta})$ to the sums of $\mathbf{p}$ and $\mathbf{k}$. Since all other factors are even in $\mathbf{p}$ and $\mathbf{k}$, this means that the first nonvanishing term in (D9a) has both k^2 and p^2, or two extra factors of T, since each k or p factor contributes $T^{1/2}$ to $\sum_{p,k}n_pn_kF(p,k)$. Thus (D9a) is at least of order T^5. However, to lowest order in T (D9b) gives

$$\frac{2}{N^3}\sum_{pkq}n_pn_k\frac{-2\epsilon_q/2S}{-2\epsilon_q}=\frac{2n_0^2}{2S}. \qquad \text{(D11)}$$

One sees that the rest of (D9b) is of order T^5 from the fact that the difference between $V[\frac{1}{2}(p-k),q+\frac{1}{2}(p-k),\ p+k]$ and $V[q+\frac{1}{2}(p-k),\ \frac{1}{2}(p-k),\ p+k]$ is just equal to $(2s)^{-1}(\epsilon_k+\epsilon_p-\epsilon_{k-q}-\epsilon_{p+q})$, so that the contributions of (D9a) and (D9b) differ only by the $2n_0^2/2s$ term. Since we have already seen that (D9a) is of order T^5, (D9b) must equal $(2n_0^2/2S)+O(T^5)$. Neglecting all higher-order terms, which we will show are of order T^5, we have then

$$\frac{1}{N}\sum_k\langle S_k^+S_k^-\rangle=\frac{2S}{N}\sum_k\langle a_k^+a_k\rangle-2n_0^2(1-1/2S)+O(T^5). \qquad \text{(D12)}$$

To see that the higher-order terms can be neglected up to order T^5, consider any diagram of the form of Fig. 18(a). By the arguments already given, only the contributions of diagrams like (D9b) with the backward line vertex on the right need be considered, since all others are of order T^5. The second term in the series is given in Fig. 18(b), and its contribution is proportional to

$$\frac{1}{N^4}\sum_{pkqq'}n_pn_k\frac{V[\frac{1}{2}(p-k),\ q+\frac{1}{2}(p-k),\ p+k]V[q+\frac{1}{2}(p-k),\ q'+\frac{1}{2}(p-k),\ p+k]}{(\epsilon_k+\epsilon_p-\epsilon_{k-q}-\epsilon_{p+q})(\epsilon_k+\epsilon_p-\epsilon_{k-q'}-\epsilon_{p+q'})}.$$

That this is of order T^5 is apparent from two facts. First of all, the lowest-order contribution is obtained from setting $\mathbf{p}$ and $\mathbf{k}$ equal to zero, and vanishes since $\sum_qV(q,q',0)=0$. Second, using the exact same reasoning as before, replacing $V[\frac{1}{2}(p-k),\ q+\frac{1}{2}(p-k),\ p+k]$ by $V[q+\frac{1}{2}(p-k),\ \frac{1}{2}(p-k),\ p+k]$ introduces a correction that vanishes according to our first statement

$$(\sum_qV(q,q',0)=0).$$

But when we have $V[q+\frac{1}{2}(p-k),\ \frac{1}{2}(p-k),\ p+k]$ in the numerator, the contribution is of order T^5. Since all higher-order terms have the above factor multiplying them, they may be neglected also. Thus we conclude that Eq. (D12) is valid. Since this is identical to Eq. (D3), we conclude that our approximate Green's function reproduces the Dyson-Wortis results to all orders in $1/S$.

[41] Actually, the diagrams we are considering have not been explicitly treated in the literature. However, the formalism of Bloch and DeDominicis for the free energy is extremely close to that required. Their results may be taken over if one connects the four free lines to a "dummy" vertex, which has matrix element unity. This is described by A. B. Harris [J. Phys. Chem. Solids **28**, 1579 (1967)] and the result we will obtain is derived there to lowest order in T.